FORMATION OF AIR-ENTRAINING VORTICES AT HORIZONTAL
WATER INTAKES

A THESIS SUBMITTED TO
THE GRADUATE SCHOOL OF NATURAL AND APPLIED SCIENCES
OF
MIDDLE EAST TECHNICAL UNIVERSITY

BY

CİHAN ZALOĞLU

IN PARTIAL FULFILLMENT OF THE REQUIREMENTS
FOR
THE DEGREE OF MASTER OF SCIENCE
IN
CIVIL ENGINEERING

AUGUST 2014

Approval of the thesis:

FORMATION OF AIR-ENTRAINING VORTICES AT HORIZONTAL WATER INTAKES

submitted by **CİHAN ZALOĞLU** in partial fulfillment of the requirements for the degree of **Master of Science in Civil Engineering Department, Middle East Technical University** by,

Prof. Dr. Canan Özgen   _____
Dean, Graduate School of **Natural and Applied Sciences**

Prof. Dr. Ahmet Cevdet Yalçıner   _____
Head of Department, **Civil Engineering**

Prof.Dr. Mustafa Göğüş   _____
Supervisor, **Civil Engineering Dept., METU**

Examining Committee Members:

Prof. Dr. Nevzat Yıldırım   _____
Civil Engineering Dept., Gazi University

Prof. Dr. Mustafa Göğüş   _____
Civil Engineering Dept., METU

Prof. Dr. Zafer Bozkuş   _____
Civil Engineering Dept., METU

Assoc. Prof. Dr. Mehmet Ali Kökpınar   _____
TAKK Dept., State Hydraulic Works

Assoc. Prof. Dr. Mete Köken   _____
Civil Engineering Dept., METU

                                                Date: 11.08.2014

I hereby declare that all information in this document has been obtained and presented in accordance with academic rules and ethical conduct. I also declare that, as required by these rules and conduct, I have fully cited and referenced all material and results that are not original to this work.

Name, Last name: Cihan ZALOĞLU

Signature: _____

ABSTRACT

FORMATION OF AIR-ENTRAINING VORTICES AT HORIZONTAL WATER INTAKES

ZALOĞLU, Cihan

M.S., Department of Civil Engineering

Supervisor: Prof. Dr. Mustafa GÖĞÜŞ

August 2014, 86 pages

The goal of this study is to estimate the critical submergence depths of horizontal water intakes that have symmetrical and asymmetrical approach flow conditions by using empirical equations. Therefore a series of experiments were performed in a reservoir-pipe system dominated by gravity and controlled by a valve. On account of adjustable lateral walls, symmetrical and asymmetrical flow conditions were created at various Froude numbers. For a wide range of discharges and for three different pipe diameters, the critical depths of air-entraining vortices were observed. These observations were evaluated by dimensional analysis and dimensionless parameters were suggested. Finaly empirical equations were derived and the results were compared with similar studies in the literature

Keywords: Horizontal intakes, Air-entraining vortices, Critical submergence.

ÖZ

YATAY SU ALMA YAPILARINDA HAVA SÜRÜKLEYİCİ VORTEKSLERİN OLUŞUMU

ZALOĞLU, Cihan

Yüksek Lisans, İnşaat Mühendisliği Bölümü

Tez Yöneticisi: Prof. Dr. Mustafa GÖĞÜŞ

Ağustos 2014, 86 sayfa

Bu çalışmanın amacı simetrik ve asimetrik yaklaşım akışı koşullarındaki yatay su alma yapılarının kritik batıklık derinliklerinin ampirik denklemler kullanarak tahmin edilmesidir. Bunun için yerçekimiyle işletilen, vana ile kontrol edilen bir depo-boru sisteminde bir seri deney yapılmıştır. Ayarlanabilir yanal duvarlar sayesinde farklı Froude sayılarında simetrik ve asimetrik akım şartları yaratılmıştır. Geniş bir aralıktaki debi ve üç farklı boru çapı için hava sürükleyici vortekslerin kritik derinlikleri gözlemlenmiştir. Bu gözlemler boyut analiziyle değerlendirilmiş ve boyutsuz parametreler ortaya konmuştur. Son olarak ampirik denklemler türetilmiş ve sonuçlar literatürdeki benzer çalışmalarla karşılaştırılmıştır.

Anahtar Kelimeler: Yatay su alma yapıları, Hava sürükleyici girdaplar, Kritik batıklık.

To my wife and family…

ACKNOWLEDGEMENTS

This humble piece of academic study would not be prepared without guidance. For this reason Prof. Dr. Mustafa GÖĞÜŞ, supervisor of this thesis, please kindly accept my sincere appreciation and gratitudes.

Since the experimental setup required tender attention in order to be run precisely, I hereby thank you, the technicians of METU Hydromechanics Laboratory, for your clean and skillful work.

Although the experiments could be performed only by one person, it seemed to me that I could not turn a single round of a valve without her. She was there when I had hard times to breath in the lab. during hot waves of last summer and freezing in front of the setup waiting for that little vortex to be formed. She is my best friend, soulmate and most trusted colleague. Dear my wife, Deniz ZALOĞLU, thank you for your support and your believe in me.

This thesis study was a part of a greater effort that took two years and seven courses too. I must admit that, during this effort I took her as an example for her approach to courses, attitude exhibited to instructors and sincerity shown to friends. Therefore Ezgi KÖKER thank you for your help during courses and wishing you success in your academic life.

Despite many people that criticized my graduate study for being irrelevant regarding to my business occupation, they were my strongest supporters, self sacrificing mothers, guiding fathers and cheerful brothers. Nezahat ZALOĞLU, Gürcan ZALOĞLU, Hakan ZALOĞLU, Hesna ŞEN, Muzaffer ŞEN and Anıl ŞEN, I very much thank you for being my family and not refusing to give your endless love and support.

TABLE OF CONTENTS

x

LIST OF TABLES

LIST OF FIGURES

FIGURES

xv

LIST OF SYMBOLS

a   Intake gate height

b   Horizontal distance from the center of the intake to a side wall of the reservoir

b1   Horizontal distance from the center of the intake to the left side plexiglass wall

b2   Horizontal distance from the center of the intake to the right side plexiglass wall

c   Vertical distance between the lowest point of the intake pipe and reservoir bottom

c1   Regression variable

c2   Regression variable

c3   Regression variable

c4   Regression variable

Di   Intake diameter

Fr   Intake Froude number

g   Gravity acceleration

h   The depth of water above centerline of the intake

H   Submergence for vertical intakes

Ko   Intake Kolf number

Γ Average circulation imposed to flow

Qi   Intake discharge

R   Correlation coefficient

Re   Intake Reynolds number

Re_R Radial Reynolds number

Sc   Critical submergence measured from the summit point of horizontal intakes

Sc*	Critical submergence measured from the center of horizontal intakes
V_i	Average velocity of the flow at the intake pipe
ν	Kinematic viscosity of water
ρ	Density of the fluid
μ	Dynamic viscosity of the fluid
σ	Surface tension of the fluid
We	Intake Weber number

CHAPTER 1

PREAMBLE

1.1. IMPORTANCE OF ESTIMATING THE FORMATION OF VORTICES AT INTAKE STRUCTURES

In near future, according to many political experts potable water is expected to be held responsible for many clashes between neighbouring countries around the world. That would occur because this valuable resource is getting contaminated or harder to be accessed. In this era, nobody wants to waste neither one drop of water potantial nor excess one cent to utilize it. Since water supply was one of the main reasons of civil engineering to be born, many design criteria have been constituted up to the present. One of the major criteria is about optimization between the cost and depth of horizontal intakes that take water to conveyence channel or tunnel etc. As per the negative effects of vortices like loss of discharge capacity, hydromechanical equipment damage due to cavitation, these intakes are wanted to be arranged so that there would be enough water height above the intake to avoid air-entraining vortices. On the other hand any attempt to increase the depth of the intake would mean an increase in the cost of retaining or storage structures. Therefore estimating the water depths at which vortices will form is important in order to optimize the cost and the effectiveness and safety of these hydraulic structures.

1.2. CRITICAL SUBMERGENCE

The depth under which the intake is submerged in water, is known as "submergence". What makes this depth "critical" is the moment when the water level reaches that point, occurance of air-entraining votices become indisputably often. During this study it is seen that even if the water level did not reach the critical depth for relevant intake, some "random" vortices could be formed instantly. Although all vortices are random events, the observations in this study show that when the water level converges to significant level, the increase in symptoms of vortex like disturbance on the water surface and formation of dimples etc. could be seen clearly and the vortex occurance depth could be estimated. In this regard, the randomness of the above mentioned vortices come from their occurance showing no symptoms at all.

1.3. TRIGGERS OF VORTICES

The common prevailing opinion in literature is that any asymmetrical flow condition towards an intake structure would increase the probability of vortex formation with respect to symmetrical flow conditions. Likewise Durgin & Hecker (1978) put forward three fundamental vorticity sources as shown in Figure 1.1. Their opinion is that these vortices are mainly initiated by: eccentric orientation of the intake relative to a symmetric approach flow, existence of shear layers of high velocity gradients, rotational wakes created by obstructions.
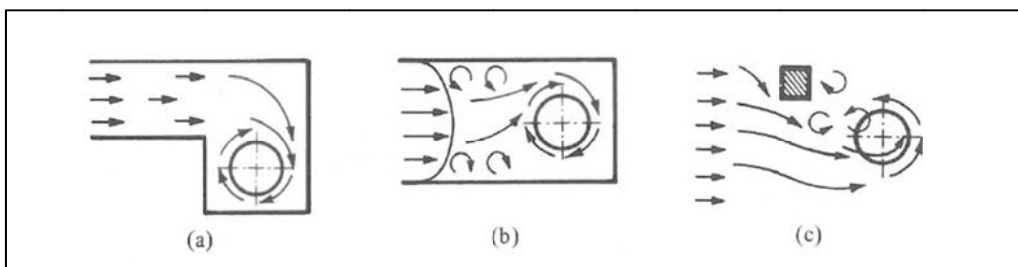
Figure 1.1 Vorticity sources (a) offset introduction, (b) velocity gradients, (c) obstruction (Durgin and Hecker, 1978)

2

1.4. HARMS OF VORTICES

According to Knauss (1987) there are two main drawbacks of presence of vortices at intake structures from hydraulics point of view; vibration on hydromechanical equipments and harms of cavitation on pressured conveyance structures. The breakdown of the main difficulties arised from vortices are given below;

- Increased head loss rise,
- Losing intake discharge,
- Losing efficiency of hydromechanical equipment due to low discharge,
- Some troubles at hydromechanical equipment due to disturbed flow pattern,
- Rigour of vibration and cavitation on hydromechanical equipment due to air-ingestion.

1.5. CLASSIFICATION OF INTAKES

As air-entraining vortices begin to occur at the free surface and reach out the intake, the type of the intake plays a great role at the classification of them. Intakes may be named regarding their reception direction and structure that hosts the intake. Figure 1.2 shows this classification. The critical submergence for horizontal intakes is generally denoted as S_c.
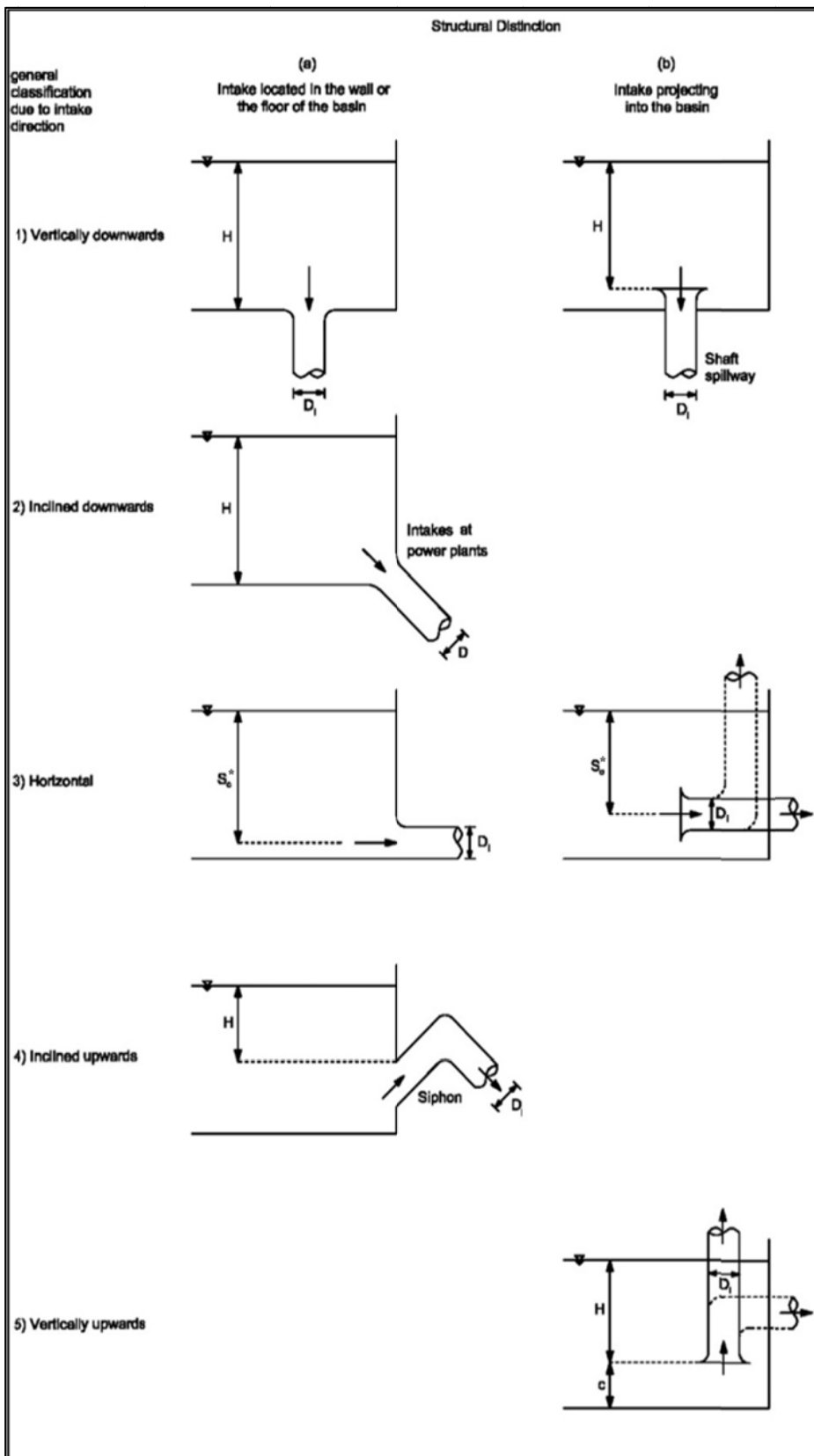
Figure 1.2 Classification of intake structures (Knauss, 1987)

1.6. KINDS OF VORTICES

Vortices can be either on the free water surface or under the water surface. Since the vortices that occur on the free surface have contact with air, these vortices can easily entrain air into their swirl core and carry it to the intake.

Another classification issue is the strength of vortices. Due to general occurance, dimensions of vortices are too small relative to inlets so that there is no reliable way of measuring the strength parameters of these vortices. For this reason, the kind of vortices are generally determined by subjective visual observations.

Knauss (1987), mentioned the visual classification methodology of Alden Research Laboratory, ARL, which used the terms like swirl, eddy, dimple and vortex tail. Formation steps of vortices include these terms and can be seen in Figure 1.3. If the surface vortices are in question, the order of formation starts with a small swirl then lingering to a dimple followed by development of a tail and reaching to the intake.
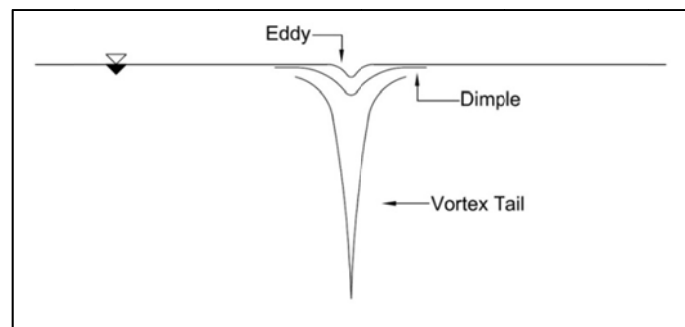
Figure 1.3 Visual comparison of eddy/swirl, dimple and vortex tail related to their strength

Details of surface vortex formation steps related to ARL are explained below (Figure 1.4):

    1.   Observation of swirling at the free water surface.

5

2. Relatively fast turning swirlings grow to a dimple.

3. In type 3 vortex, vortex tail could only be seen by introducing dye to the vortex core.

4. Before entraining air inside, vortices can suck in free floating trash to the intake.

5. As the vortices gain strength, after the trash pulling stage, they capture air in bubles and carry to the intake.

6. A full air-cored vortex forms a funnel at the free water surface and extents continously its tail to the intake.
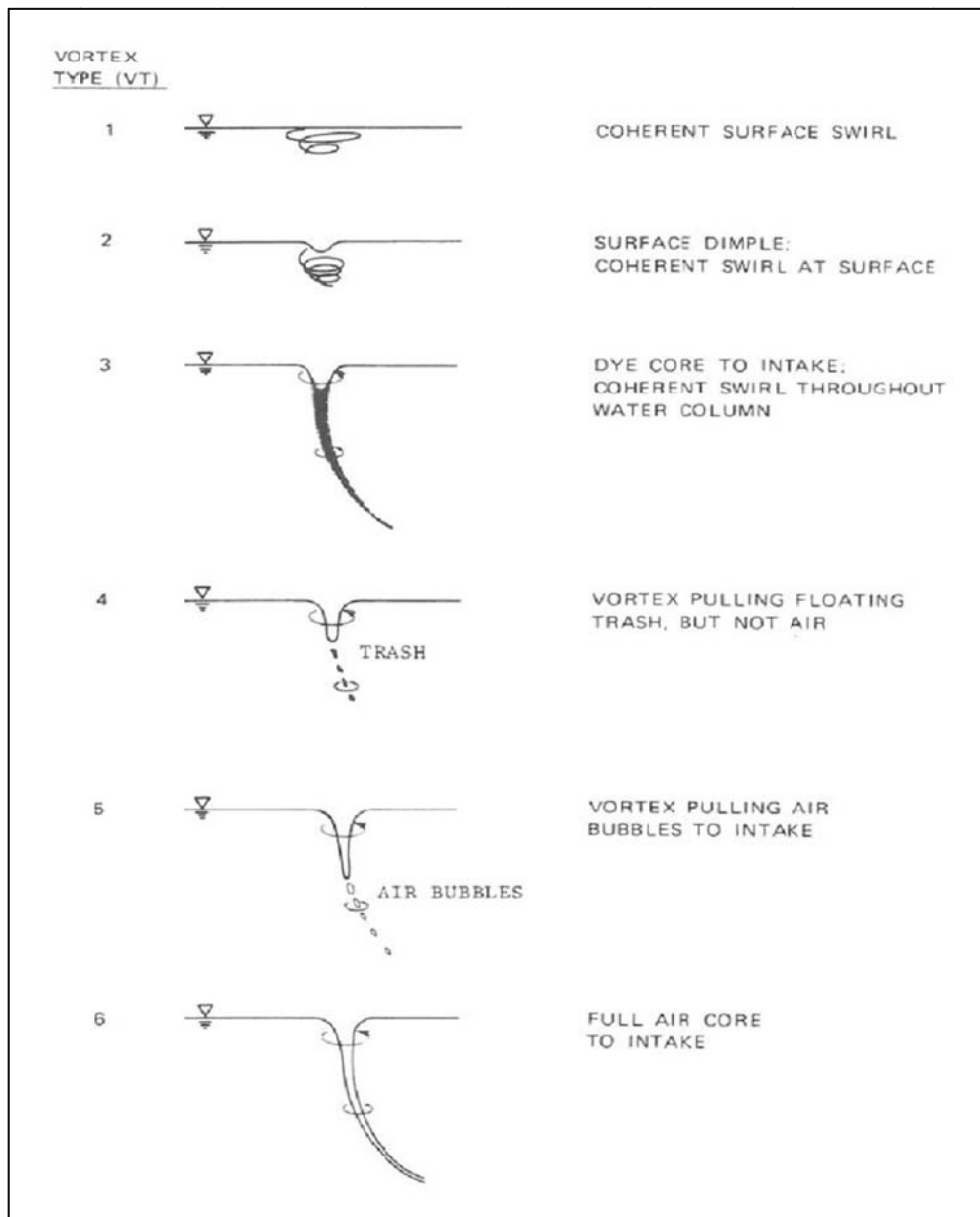
Figure 1.4 ARL vortex type classifications (Knauss, 1987)

1.7. SCOPE OF THE STUDY AND OUTLINE OF THE THESIS

The goal of this study is to estimate the critical submergence depths of horizontal water intakes that have asymmetrical reception geometry as well as symmetrical by deriving empirical equations. Therefore a series of experiments were performed in a reservoir-pipe system dominated by gravity and controlled by a valve. In order to observe the formation routine and the behaviour of air-

entraining or full air core (Type 6) vortices, a hydraulic model was prepared. This model was able to simulate symmetrical and asymmetrical flow geometries by adjustable lateral walls and giving chance to imitate different flow conditions for calculating dimensionless parameters, like Froude number, by controllable discharge and 3 different horizontal intake pipe diameters. This study started with a literature review which is presented in Chapter 2. It is the Chapter 3 that includes the dimensional analysis for the model was performed to determine the influential dimensionless parameters on the air-entraining vortices for horizontal pipe intakes. The experimental setup and how the experiments were performed are described at Chapter 4. After this part, the experimental results are processed to graphs and empirical formulas for the critical submergence of horizontal pipe intakes and compared to previous studies in Chapter 5. At the end a final discussion and conclusion is given in Chapter 6.

CHAPTER 2

LITERATURE SURVEY

Estimating the behaviour of vortex formation has been a great source of attention among hydraulic society and many studies have been done via analytical and numerical methods. These analytical approaches include different intake geometries, boundaries and approach conditions creating different parameters. As these parameters are discussed, some of them can be said to have minimum or no effect on vortex formation. Customization of these analytical models are very difficult as per the unique conditions of the real cases. Theoretically vortex formation is a complex phenomena to be dealt with yet can be simplified by some assumptions allowing mismatching of model and real cases. For the sake of reliability of real cases, physical models are widely recommended.

Anwar (1965, 1967 and 1968) had studies on steady vortices occuring at the entrance of an outlet pipe. Experiments were run inside a cylindrical tank having a vertical intake pipe. Consequent of these experiments revealed that if the radial Reynolds number $Re_R = Q_i/\nu H$, where Q_i is the volumetric flow rate, H is the vertical intake submergence and ν is the kinematic viscosity of water, is greater than 10^3, effect of viscosity can be omitted.

Gordon (1970) studied 29 running hydroelectric intakes to build a design criteria to avoid air entraining vortices on low head intakes. The main parameters were assumed as geometry of the approach flow, velocity at the intake, the size of the intake and the submergence. Since intake geomety differs from case to case, to concentrate on other parameters rather than intake

geometry was decided. The following formulas were derived to show the relation between the critical submergence and Froude number;

$$\frac{S_c}{D_i} = 1.70Fr \qquad\qquad 2.1$$

for symmetrical approach flow conditions and,

$$\frac{S_c}{D_i} = 2.27Fr \qquad\qquad 2.2$$

for asymmetrical approach flow conditions, where S_c is the critical submergence depth which is measured from the summit point of the intake and Fr is the intake Froude number ($Fr = V_i/\sqrt{gD_i}$)

Reddy and Pickford (1972) introduced a design criteria to prevent vortices in pump sumps and at horizontal intakes. They defined the critical submergence as a function of Froude number, Reynolds number and a wave parameter. Since vortex formation was a free water surface event, wave length and Reynolds number were neglected leaving Froude number to be the main parameter. They suggested a sufficient submergence having no vortex can be calculated by below formulation;

$$S_c/D_i = 1 + Fr \qquad\qquad 2.3$$

for both hydroelectric practice and pump sumps.

Daggett and Keulegan (1974) investigated effects of surface tension and viscosity on vortices and explained similarity conditions between hydraulic structures and their models on critical submergence, vortex shape, size and efficiency of the outlet structure. Two different scaled cylindrical tanks with various diameters of vertical outlet pipes, liquids and vane angles were used.It was concluded that after a certain value of Re, influence of viscosity dropped and the only important parameter grew as the circulation number.

10

Zeigler (1976) made a hydraulic model of Grand Coulee Third Powerplant to investigate vortex safety of penstock. It came out that increasing the amount of operating units in small discharges causes increase in vortex strength.

Anwar et al. (1978) studied on air-entraining vortices at horizontal intakes.Experimental results revealed that effect of viscous forces and surface tension can be ignored throughout the formulation when radial Reynolds number and Weber number are greater than a certain value. So, other parameters such as circulation number and Froude number remain in control of the formulation.

Gulliver and Rindels (1983) gathered up-to-date data on intakes having vortex problems and presented in Figure 2.1. It can be interpreted that neither Gordon's (1970) criteria nor Reddy and Pickford (1972) design criteria is quite successful to represent the critical case.
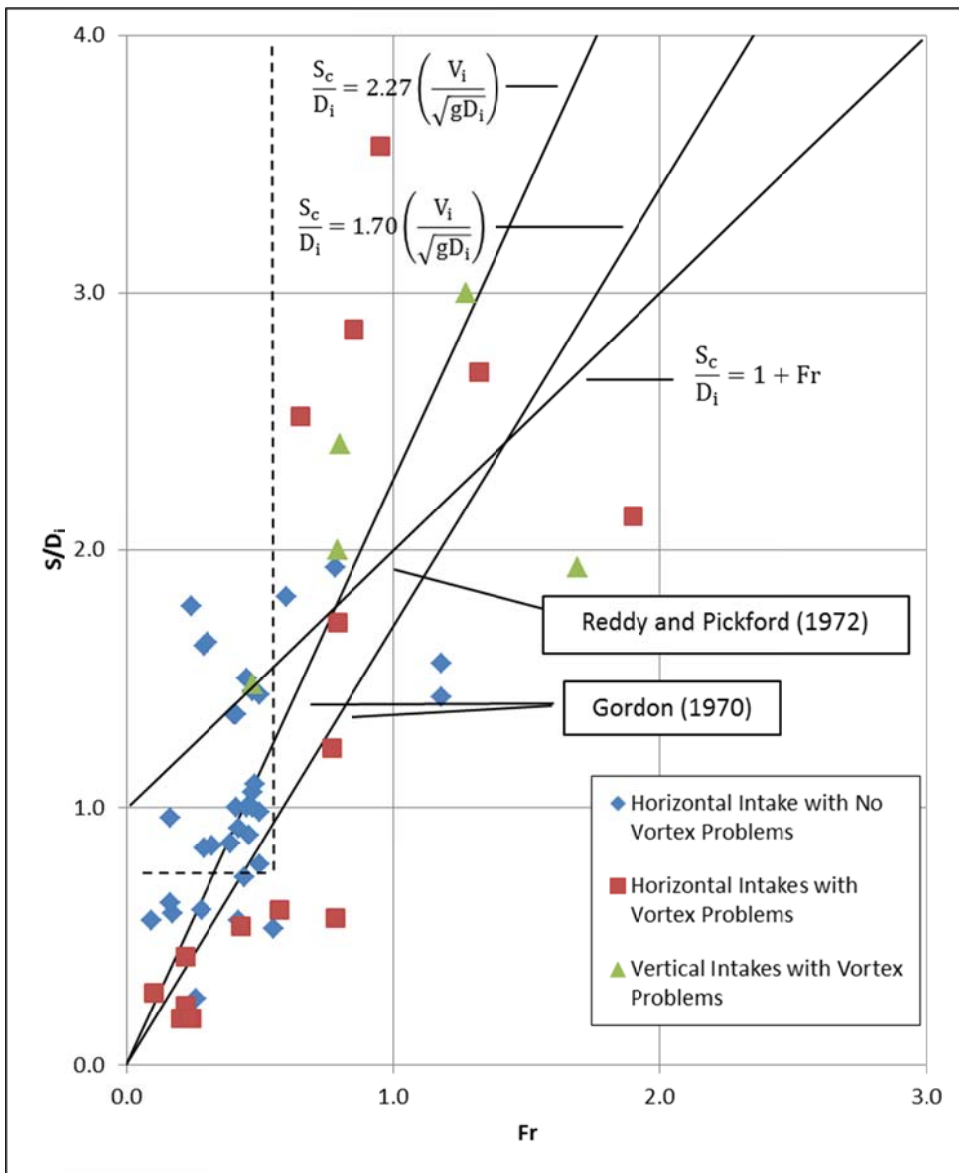
Figure 2.1 Dimensionless plot of data obtained from existing intakes, field installations and model studies (Gulliver and Rindels, 1983)

Knauss (1987) studied some large size intakes of powerplants and recommended a submergence depth of 1 up to 1.5 times the intake diameter. It is given that the submergence requirements may be found using the formula given in Figure 2.2.
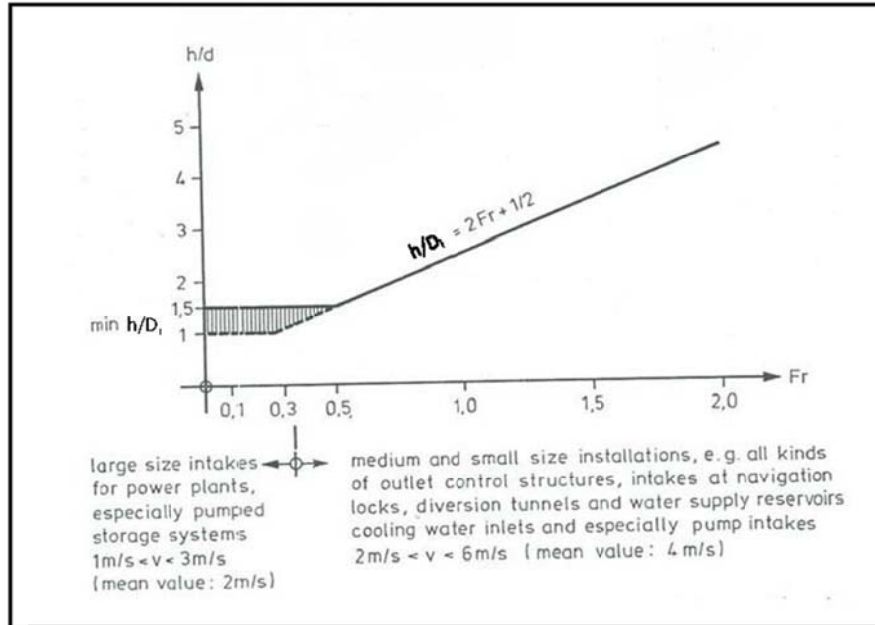
Figure 2.2 Recommended submergence for intakes with proper approach flow conditions, (Knauss, 1987)

Yıldırım and Kocabaş (1995) studied on occurance behaviour of air-entraining vortices in a horizontal rectangular flume through a vertical intake. They used Rankine's half body approach to explain the critical submergence need of an intake.

Jiming et al (2000) performed experiments on a double and a single intake for determination of critical submergencies by using a large scale hydraulic model. Consequently they presented two empirical equations for both symmetrical and non-symmetrical flow conditions as follows;

$$\frac{S_c}{a} = 2.39 Fr - 0.001 \qquad\qquad 2.4$$

for symmetrical approach flow and,

13

$$\frac{S_c}{a} = 3.17Fr - 0.001 \qquad\qquad\qquad 2.5$$

for non-symmetrical approach flow where a stands for intake gate height. Equation 2.3 was compared with Gordons' formula and it was seen that Gordon formula gives lower submergences than the required submergence. That's why, Gordons' formula was suggested to be multiplied with a larger coefficient or a model study of large projects should be conducted.

Yıldırım et al. (2000) studied how the flow boundary effects the critical submergence. They carried out experiments using a horizontal intake pipe connected to a rectangular flume having a dead-end wall. They found out that the clearance between the intake pipe and dead-end wall plays a key role in vortex formation and continuity.

Ahmad et al (2008) were interested in determining critical submergence for 90° horizontal intake in an open channel flow. By using critical spherical sink surface theories and potential flow, an analytical equation was derived. This equation was compared to model experiment results but failed to comply. This non-compliance was discussed over large boundary effect and ignorance of viscosity, surface tension and circulation effects from the analytical equation.

Gürbüzdal (2009) carried out a series of experiments over four different diameters of horizontal intake pipes for possible scale effects on vortex formation. Froude number, Reynolds number and side wall clearance were chosen as the important dimensionless parameters and an empirical formula, Equation 2.6, was derived from the experimental results.

$$\frac{S_c}{D_i} = Fr^{0.865}\left(\frac{b}{D_i}\right)^{-0.565}Re^{0.0424} \qquad\qquad 2.6$$

Where b is the side wall clearance measured from the centre of the intake. Equation 2.6 is valid for $0.51 \leq Fr \leq 4.03$, $1.597 \leq b/D_i \leq 5.147$ and

$2.96x10^4 \leq Re \leq 2.89x10^5$ (Re = $V_i D_i \rho / \mu$). It was observed that S_c/D_i becomes independent of b/D_i for $b/D_i \geq 6$

Yıldırım et al (2009) concentrated on how the positions of two vertical intakes effect the critical submergence of the system. The experiments showed the critical submergence of the dual intakes is greater than a single intake pipe because, with dual intakes, there is more disturbance which triggers vortices.

Taştan and Yıldırım (2010) focused on the effects of dimensionless parameters and, boundary friction on air-entraining vortices and the critical submergence of a vertically directed intake for the cases of no-circulation imposed cross-flow and still water. They found that for cross-flow, there are certain limiting values of Fr, Re, and We (We = $\rho V_i^2 D_i / \sigma$) and beyond these values S_c is independent of them.

Baykara (2013) studied on air-entraining vortices for what hydraulic conditions cause them and what are the precautions to prevent or mitigate the effects by testing anti-vortex devices. Some different horizontal intake pipe diameters and symmetric side wall clearences were tested to gather dimensionless flow parameters like Fr, Re and We into an equation for critical submergence. Moreover, anti-vortex plates were tested for some discharge values to show the relation of plate dimensions and vortex occurance. If the experiments are reviewed in detail, it could be seen that six different intake pipes having diameters 30, 25, 19.4, 14.4, 10, 5 cm were used. The setup had six different symmetrical side wall clearances 2b= 40, 60, 80, 100, 120 and 140cm. These pipes yield $2b/D_i$ values varying from 1.33 to 16.00. The data set was divided into three groups as maximum, minimum and intermediate values of S_c/D_i. Also a region of data that shows no dependency of S_c/D_i on $2b/D_i$ was described. The empirical equations presented in that study are as follows;

For maximum values of S_c/D_i, $1.33 \leq 2b/D_i \leq 4.00$,

$$\frac{S_c}{D_i} = Fr^{5.792}Re^{3.246}We^{-4.333}\left(\frac{2b}{D_i}\right)^{-3.489} \qquad 2.7$$

For minimum values of S_c/D_i, $2.00 \leq 2b/D_i \leq 8.00$,

$$\frac{S_c}{D_i} = Fr^{0.039}Re^{-0.357}We^{-0.425}\left(\frac{2b}{D_i}\right)^{-0.602} \qquad 2.8$$

For intermediate values of S_c/D_i, $3.33 \leq 2b/D_i \leq 12.00$,

$$\frac{S_c}{D_i} = Fr^{0.336}Re^{-0.229}We^{0.401}\left(\frac{2b}{D_i}\right)^{-0.261} \qquad 2.9$$

After removing the parameters of Re, We, $2b/D_i$ Equation 2.9 is given as below,

$$\frac{S_c}{D_i} = Fr^{0.639} \qquad 2.10$$

In the zone of the data where S_c/D_i is independent of $2b/D_i$, the general form of S_c/D_i is expressed as below,

$$\frac{S_c}{D_i} = Fr^{0.324}Re^{-0.176}We^{0.282} \qquad 2.11$$

After ignoring the terms of Re and We, Equation 2.11 is reduced to the form given in Equation 2.12.

$$\frac{S_c}{D_i} = 1.278\, Fr^{0.558} \qquad 2.12$$

16

CHAPTER 3

MODELLING OF AIR-ENTRAINING VORTICES

3.1. INTRODUCTION

Air-entraining vortices are results of some complex interaction among intake zone geometry, flow velocity and liquid properties. As a result of complex and hard to solve flow conditions of intake region, the critical submergence of intake structures are generally determined either by past experience or model studies.

3.2. DIMENSIONLESS PARAMETERS

In order to acquire the dimensionless parameters which dominate the phenomenon, dimensional analysis is applied. The variables involved into the phenomenon can be grouped as below:

Fluid Properties: Density of the fluid (ρ), dynamic viscosity of the fluid (μ), and surface tension of the fluid (σ).

Flow Properties: Average velocity of the flow at the intake pipe (V_i), average circulation imposed to flow (Γ), and gravitational acceleration (g).

Geometric Properties of the Intake Zone: Diameter of the intake pipe (D_i), the distance between the lowest point of the intake and the reservoir bottom (c), left-side (with respect to flow direction)-wall distance of the reservoir to the intake center line (b_1) and right-side-wall distance of the reservoir to the intake center line (b_2).

Considering a horizontal intake type shown in Figure 3.1, the critical submergence, S_c, (described as the safe distance between the intake and the free water surface so as to avoid air-entraining vortices) should depend on the below variables.

$$S_c = f_1 \ (\rho, \ \mu, \ \sigma, \ g, \ V_i, \ \Gamma, \ Di, \ c, \ b_1, \ b_2) \hspace{4cm} 3.1$$

where S_c is taken from the free water surface to the top of the intake pipe.
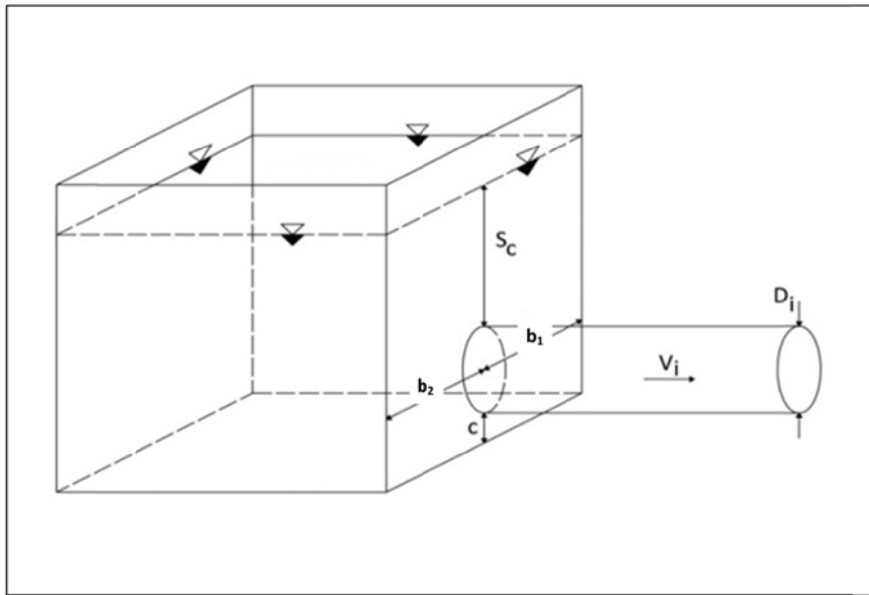
Figure 3.1 Geometric properties of the model.

After performing dimensional analysis, the related dimensionless parameters are found as below;

$$\frac{S_c}{D_i} = f_2 \left(\frac{b_1}{D_i}, \ \frac{b_2}{D_i}, \ \frac{c}{D_i}, \ Re, \ Fr, \ We, \ K_o \right) \hspace{3cm} 3.2$$

where

$$Re = \text{Intake Reynolds number} = \frac{V_i D_i \rho}{\mu}$$

$$Fr = \text{Intake Froude number} = \frac{V_i}{\sqrt{gD_i}}$$

$$We = \text{Intake Weber number} = \frac{\rho V_i^2 D_i}{\sigma}$$

$$K_o = \text{Intake Kolf number} = \frac{\Gamma}{V_i D_i}$$

Since the experimental setup does not have bottom clearance, i.e. c=0, the dimensionless term containing c can be ignored. The terms containing b_1 and b_2 are preferred to be combined as $(b_1+b_2)/D_i$ and $|(b_1-b_2)|/D_i$ for symmetrical and asymmetrical approach flow conditions, respectively. After these changes, the Equation 3.2 can be re-aranged as below;

$$\frac{S_c}{D_i} = f_2 \left(\frac{(b_1+b_2)}{D_i} \text{ or } \frac{|(b_1-b_2)|}{D_i}, Re, Fr, We, K_o \right) \qquad 3.3$$

For complete similarity, the dimensionless parameters related to the geometric properties would be the same for both the model and the prototype. On the contrary, the expecting equality of S_c/D_i for both the model and the prototype would be wrong, because all of the related dimensionless parameters Fr, Re, We, and Ko would not be equal at the same time for these two cases. Therefore, the following evaluation is made to present the importance of these parameters and give a chance to the designer to decide upon the suitable modelling criteria for his study.

3.2.1. Ignoring Kolf Number

The amount of discharge, intake type and approach geometry have effect on circulation. The dimensionless parameter Kolf number which represents the effects of circulation in Equation 3.1 can be omitted because all geometric and flow parameters are already considered in the same equation and there is no interference in the system to change the circulation. After the omission of Ko, the Equation 3.3 becomes;

$$\frac{S_c}{D_i} = f_2 \left(\frac{(b_1 + b_2)}{D_i}, \text{Re}, \text{Fr}, \text{We} \right) \qquad\qquad 3.4$$

for symmetrical approach flow conditions and,

$$\frac{S_c}{D_i} = f_2 \left(\frac{|(b_1 - b_2)|}{D_i}, \text{Re}, \text{Fr}, \text{We} \right) \qquad\qquad 3.5$$

for asymmetrical approach flow conditions.

3.2.2. Dominance of Weber Number

According to the past studies, vortices composed of weak dimples are connected to the Weber number. For instance, Anwar et al. (1978) preferred not to consider surface tension effect as it loses its dominance with respect to We number when We number exceeds a certain value. In this study, We number is seen effective over air-entraining vortices therefore it is included in the analyses.

3.2.3. Relation of Reynolds Number

Some researchers like Daggett and Keulegan (1974) and Anwar et al. (1978), tried to propose limit values for Re number that makes the relationship between Re number and vortex formation meaningful. This study also aims to show this relation so Re number term stays in the equation.

3.2.4. Influence of Froude Number

Up to the present, the Froude number is held the most responsible for influencing the vortex formation among the other dimensionless parameters. Since vortex is formed on free water surface and dominated by gravity, the Froude number should be the main influential dimensionless parameter. Consequently, any model study to be performed, should be constructed on Froude similitude. Therefore, the approach of this study followed this base and the model study was performed on Froude similitude.

20

CHAPTER 4

EXPERIMENTAL SETUP AND PROCEDURE

4.1. EXPERIMENTAL SETUP

Since this study considers horizontal intake conditions, a reservoir should be constructed. For this reason, a rectangular concrete reservoir which can be seen between Figure 4.1 and Figure 4.3, having the length, width and depth of 3.10m x 3.10m x 2.20m, respectively, was constructed. This reservoir has a dead volume, to reduce the turbulance of the incoming water. A screen made of bricks was installed at the rear side of the active volume from which water is directed towards the intake structure so as to maintain uniform flow through the water way. The plexiglass plate that had the interference with intake pipe was extended out from the reservoir by 0.30m to get good visual observations of the vortices. In order to imitate different intake geometries, portable plexiglass side walls were deployed inside the active volume. Plexiglass intake pipes having the diameters of 25.0cm, 19.4cm, 14.4cm were installed to the setup. While installing these pipes, a great dilligence was shown to get zero bottom clearence and the same centerline for each pipe to be tested.

As the experiment was dominated by gravity, to control the discharge of the flow, a valve was connected at the end of the intake pipe. After the valve, a steel pipe allows the water to flow into an open channel which ends with a rectangular sharp-crested weir. Discharge measurement was done by a needle gauge used for recording the flow depth before the weir and calibrated by an acoustic flowmeter installed on the intake pipe. The required constant water head was supplied from a large elevated tank. Additionally, a small diameter

drainage pipe was connected to the dead volume of the reservoir to make fine tuning on the water elevation.

Plan view
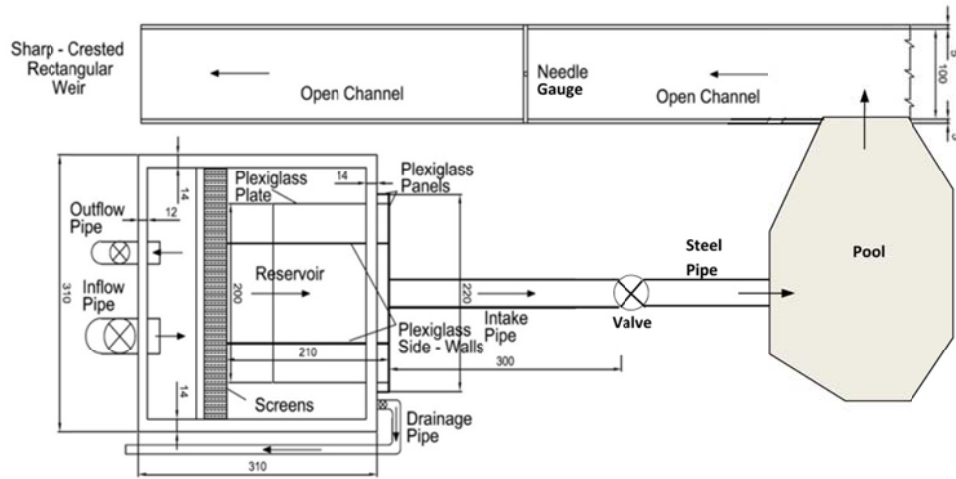
Side view
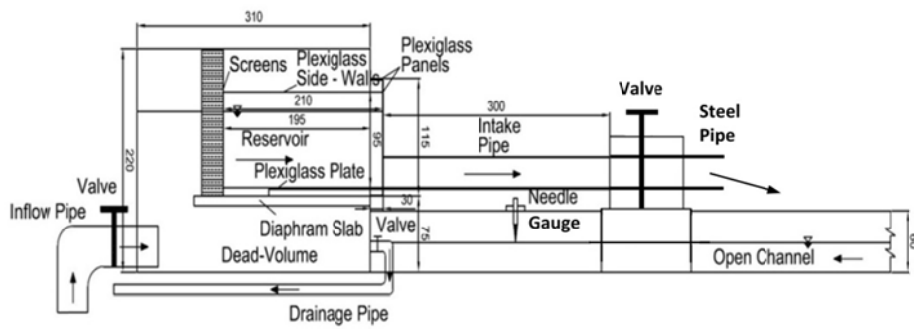
Figure 4.1 Plan and side view of the setup (dimensions are given in cm)

Figure 4.2 General view of the experimental setup (Reservoir)

Figure 4.3 General view of the experimental setup (Intake and steel pipe)

4.2. METHODOLOGY

The experimental precedure was very like the one in Baykara (2013) except the trials of asymmetrical lateral wall distances. Here again the intake pipes having diameters 25cm, 19.4cm and 14.4 cm were installed. For every diameter, 3 symmetrical and 3 asymmetrical lateral wall clearences were tested. Moreover, at least 5 to 10 different discharge values per every clearence were generated to see the critical submergence of that parameter combination. Since the water level had a limit (height of the reservoir) and the valve allowed a specific flow rate for a specific water level in the reservoir, the set of the experiments were limited between 5 to 10 (with 2 to 4 lt/s increments) discharge values. The main objective for these test runs was to obtain the certain depths when air-entraining vortices were being formed. In Appendix results of the experiments and the correlated dimensionless parameters are presented.

After getting the constant head from the elevated reservoir, every test run begun with filling the dead volume of the model reservoir. As soon as the water level filled up the active volume and reached a certain level, by opening the main valve and fine tuning from the drainage valve, the water level is allowed to drop with a constant speed. The water that left the pipe poured out to the pool and carried to the open channel where the discharge values were read. In order to maintain a constant flow rate, by monitoring via an acoustic flowmeter, the main valve was opened step by step while the water level was decreasing.

During the water level dropping, any symptom of vortex like swirls, surface disturbance, dimples and eventually vortices were observed. In case of any symptoms, the water level was fixed or rate of fall was slowed down to observe the air-entraining vortex at least two times at the same depth. Sometimes air-entraining vortices formed without these symptoms. In those cases the water level again was fixed to the exact point and water surface was observed under steady flow conditions for a considerable time, 5-10 minutes with caution.

Soon after detecting an air-entraining vortex two times at the same depth, again over a considerable period, this critical depth and the discharge calculated from the water height at the rectangular sharp crested weir, were noted down and passed to the next discharge. This single routine was performed for every intake pipe diameter, for every lateral distance combination and for every flow rate that the system allowed.

4.3. OBSERVATIONS

The critical submergence values were recorded for only the –full air core- air-entraining vortices. As a result of this every vortex symptoms classified by ARL was observed. These symptoms occurred in this order; surface disturbance, surface swirl, surface dimple, swirl throughout water column, vortex pulling trash, vortex pulling air bubbles and finally full air core vortex. Not all of the vortices were noticeable for long time. However, after passing the critical depth, all of the vortices gained strength and occurance duration.

Some of the pictures taken during experiments are shown between Figure 4.5 and Figure 4.9.

Figure 4.4 Surface dimple formation

Figure 4.5 Vortex pulling air bubbles to intake

Figure 4.6 A full air core vortex moving towards the intake

Figure 4.7 Vortex formation away from the centerline of the intake pipe

Figure 4.8 Vortex formation around the centerline of the intake pipe

Figure 4.9 Example for an air-entraining vortex

CHAPTER 5

ARGUMENTS ON THE EXPERIMENTAL RESULTS

5.1. PREAMBLE

As Equations 3.4 and Equation 3.5 are recalled; S_c/D_i was said to be related to the dimensionless parameters of $(b_1+b_2)/D_i$ or $|(b_1-b_2)|/D_i$, Re, Fr, and We. During the experiments, the necessary data like side wall clearances, pipe diameter, critical submergence, discharge and flow velocity were recorded in order to calculate the aforementioned dimensionless parameters for every set. After that, the graphs are preferred to be presented in two separate sub-groups as symmetrical and asymmetrical lateral wall clerances.

In addition, the empirical equations were obtained by regression analysis applied to these two separate sub-groups and followed by comparison to related previous studies. Summary of the symmetrical and asymmetrical experimental data is presented in Table 5.1 and Table 5.2, respectively. Addition to this, the details are given in Appendix

Table 5.1 Hydraulic and geometric parameters tested on symmetrical flow
conditions

D_i (cm)	Range of							# of Obs.
	Q_i (lt/s)	S_c/D_i	Fr	Re	We	$|(b_1-b_2)|/D_i$	$(b_1+b_2)/D_i$	
25.0	49.11 ~ 19.02	1.040 ~ 0.132	0.639 ~ 0.248	249140 ~ 96471	3432 ~ 515	0	3.200 ~ 1.600	22
19.4	49.99 ~ 15.56	2.933 ~ 0.232	1.226 ~ 0.382	326782 ~ 101745	7608 ~ 738	0	4.124 ~ 2.062	30
14.4	27.33 ~ 9.39	1.528 ~ 0.452	1.412 ~ 0.485	240712 ~ 82667	5561 ~ 656	0	5.556 ~ 2.778	20

Table 5.2 Hydraulic and geometric parameters tested on asymmetrical flow
conditions

D_i (cm)	Range of							# of Obs.
	Q_i (lt/s)	S_c/D_i	Fr	Re	We	$|(b_1-b_2)|/D_i$	$(b_1+b_2)/D_i$	
25.0	48.25 ~ 18.43	0.652 ~ 0.188	0.628 ~ 0.240	244732 ~ 93466	3311 ~ 483	0.800 ~ 0.400	2.800 ~ 2.000	21
19.4	42.66 ~ 13.93	1.557 ~ 0.263	1.292 ~ 0.342	344220 ~ 91054	8442 ~ 591	1.031 ~ 0.516	3.608 ~ 2.577	27
14.4	25.98 ~ 9.39	1.535 ~ 0.368	1.343 ~ 0.485	228793 ~ 82667	5024 ~ 656	1.389 ~ 0.694	4.861 ~ 3.472	22

5.2. SYMMETRICAL SIDE WALL CLEARANCES

5.2.1. Effect of Dimensionless Parameters on S_c/D_i

The plotted relations of the dimensionless parameters according to the experimental results are shown between Figure 5.1 and Figure 5.9. In these figures units of b_1 and b_2 are in cm.
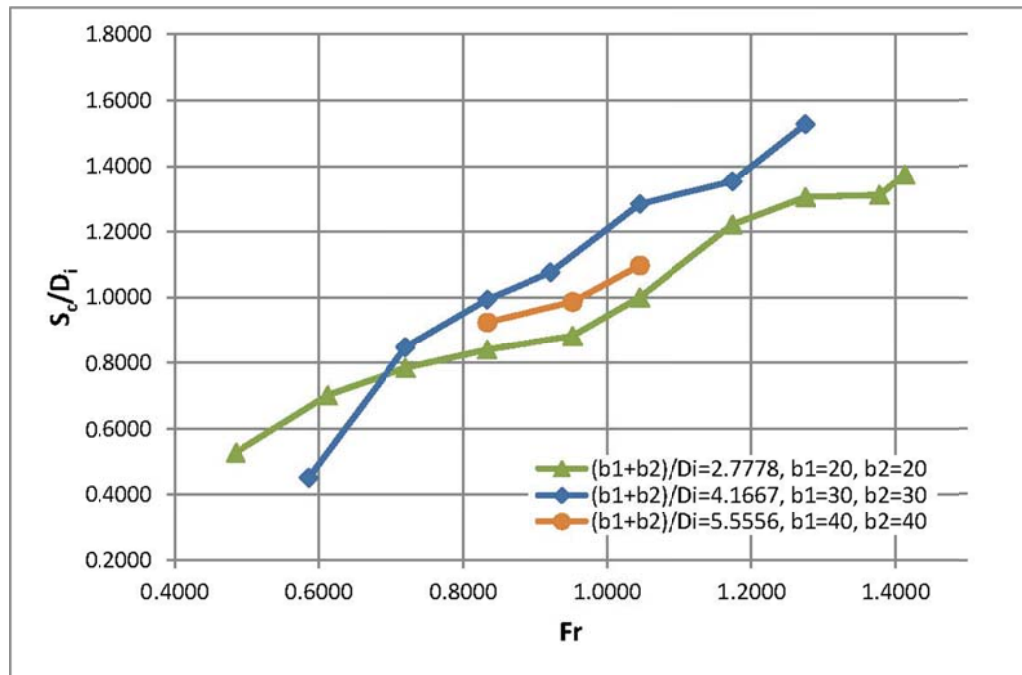
Figure 5.1 S_c/D_i versus Fr as a function of $(b_1+b_2)/D_i$ for $D_i=14.4$cm
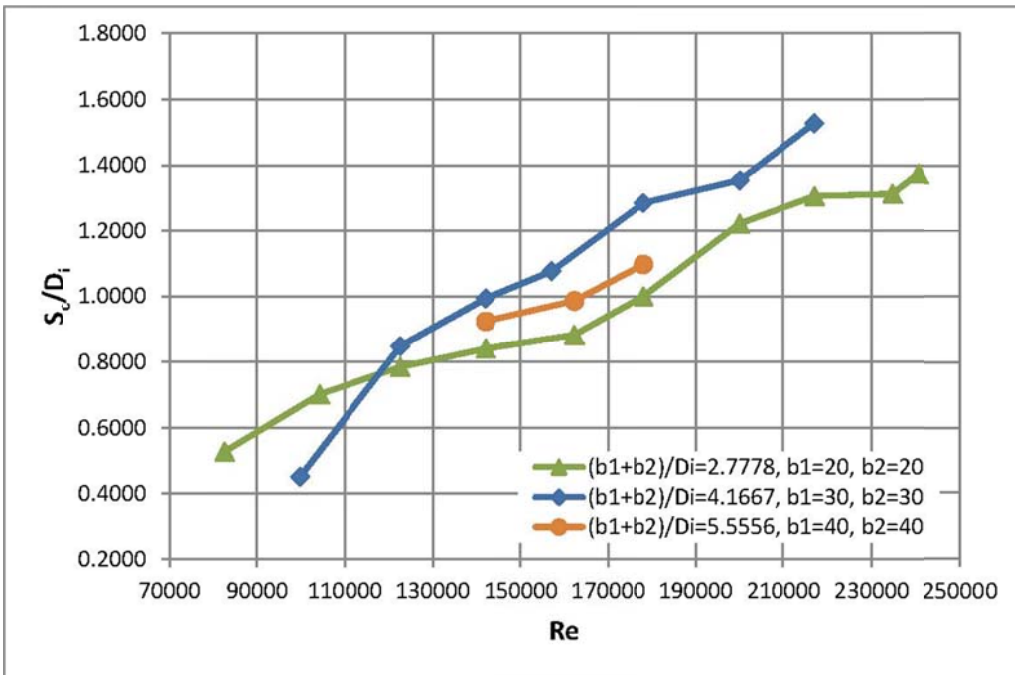
Figure 5.2 S_c/D_i versus Re as a function of $(b_1+b_2)/D_i$ for D_i=14.4cm
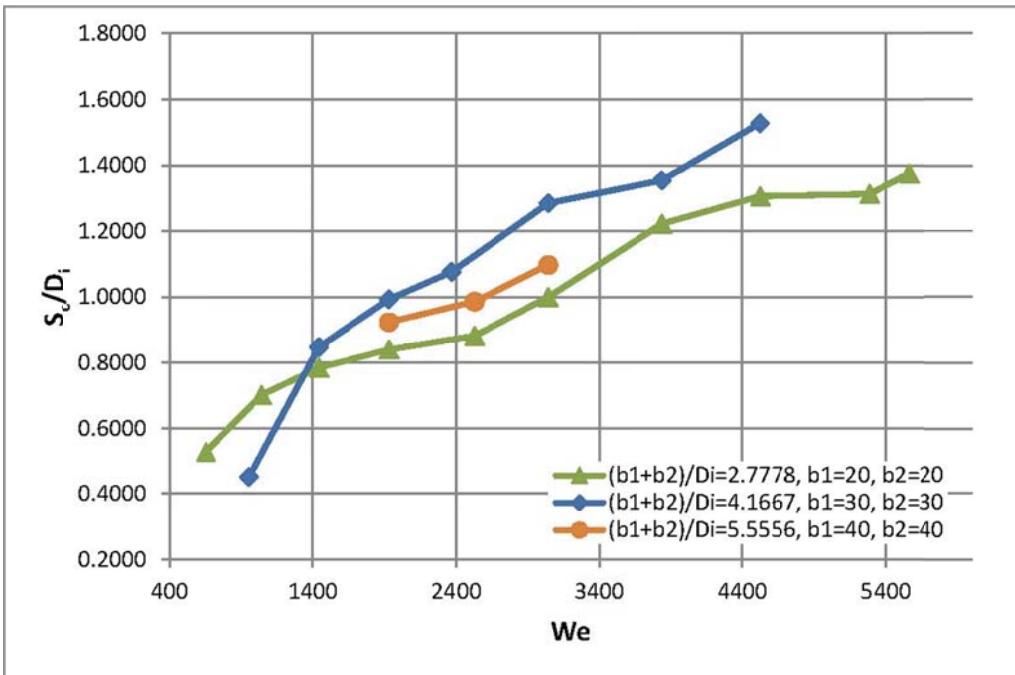
Figure 5.3 S_c/D_i versus We as a function of $(b_1+b_2)/D_i$ for D_i=14.4cm
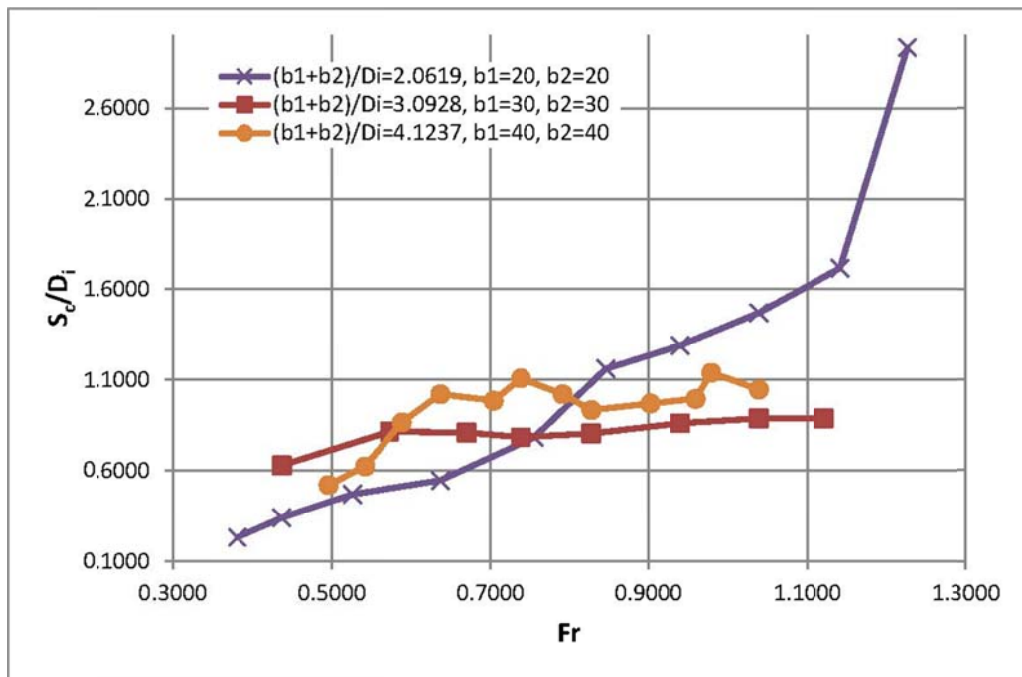
Figure 5.4 S_c/D_i versus Fr as a function of $(b_1+b_2)/D_i$ for D_i=19.4cm
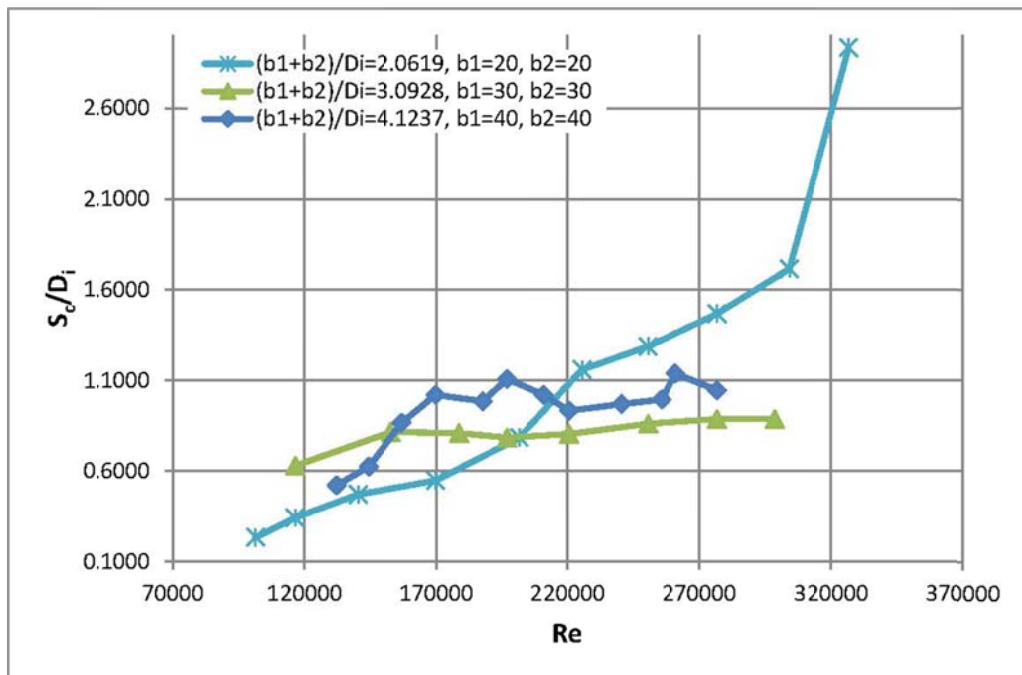
Figure 5.5 S_c/D_i versus Re as a function of $(b_1+b_2)/D_i$ for D_i=19.4cm

33
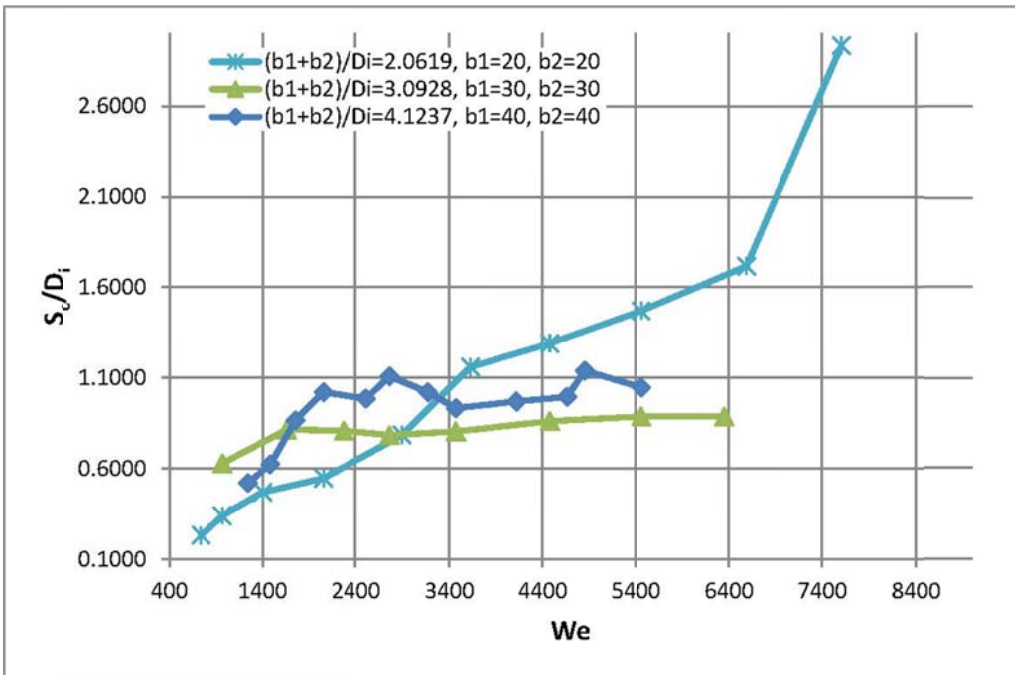
Figure 5.6 S_c/D_i versus We as a function of $(b_1+b_2)/D_i$ for D_i=19.4cm
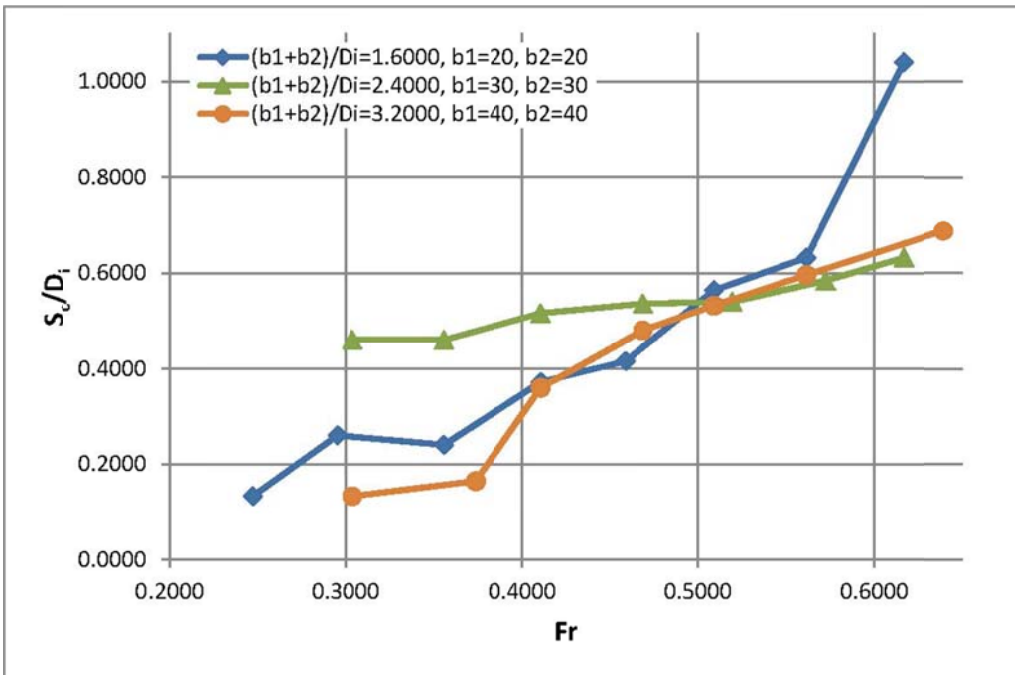
Figure 5.7 S_c/D_i versus Fr as a function of $(b_1+b_2)/D_i$ for D_i=25.0cm
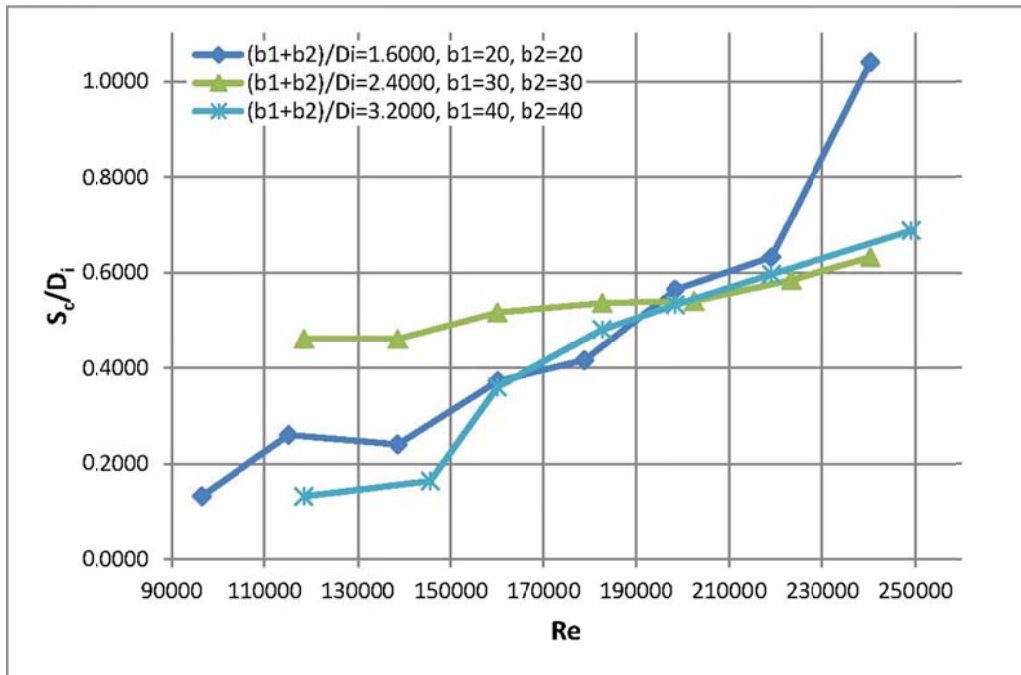
Figure 5.8 S_c/D_i versus Re as a function of $(b_{1+}b_2)/D_i$ for D_i=25.0cm
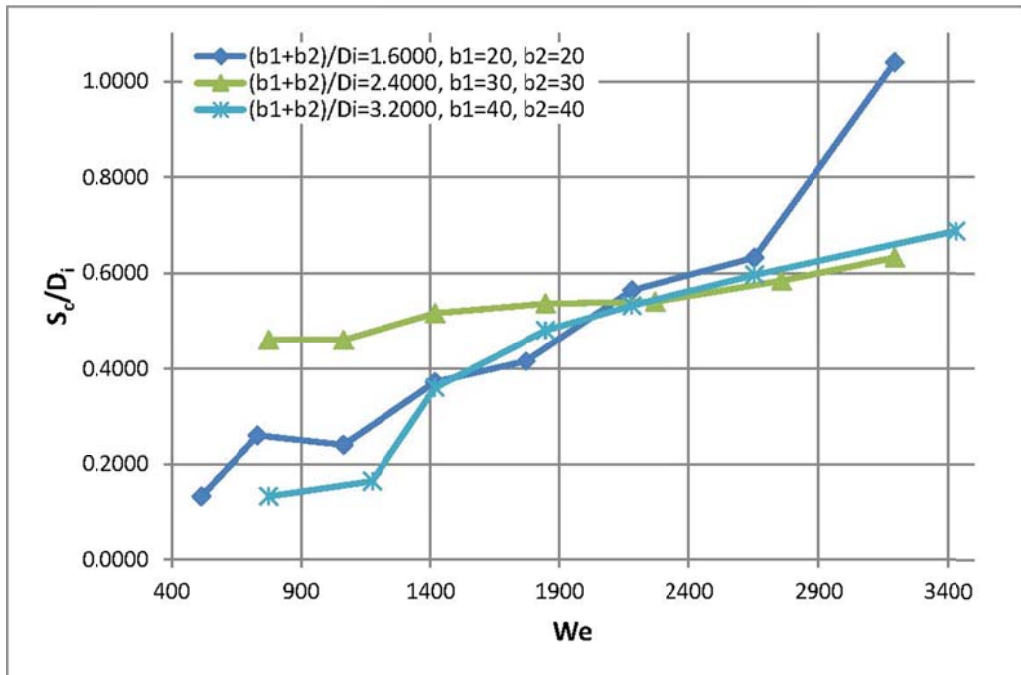
Figure 5.9 S_c/D_i versus We as a function of $(b_{1+}b_2)/D_i$ for D_i=25.0 cm

These figures can be evaluated as follows:

35

1. S_c/D_i values show increasing trend with increasing values of Fr, Re and We for a given intake diameter.

2. As the pipe diameter increases; at D_i=19.4cm and 25.0cm, the rate of change of S_c/D_i for the narrowest wall clearance; (b_1+b_2)=40cm, with the related parameters; Fr, Re, and We, increases with increasing Fr, Re, and We.

3. The curve families of $(b_1+b_2)/D_i$ generally coincide with each other at intermediate values of Fr, Re, and We tested, giving no clear relation.

5.2.2. Comparison of the Experimental Results with those of Baykara (2013)

Baykara (2013) investigated the formation of vortices on a similar model having more number of pipe diameters and side wall clearances. The outcomes of those experiments and the present ones are plotted and compared in between Figure 5.10 and Figure 5.18. In these figures units of b_1 and b_2 are in cm.

In the model used by Baykara (2013), there was a pump in the experimental setup by which the flows of high Froude numbers were achieved. In the present model there is no pump in the system and therefore, the flows of lower Froude numbers are provided. Since in practice mostly the flows of low Froude numbers are used in intake structures, the aim of this analysis is to provide more S_c/D_i data at mainly low Froude numbers and to see the general trends of the data of S_c/D_i obtained from the present and Baykara's (2013) study as a function of Fr, Re and We.
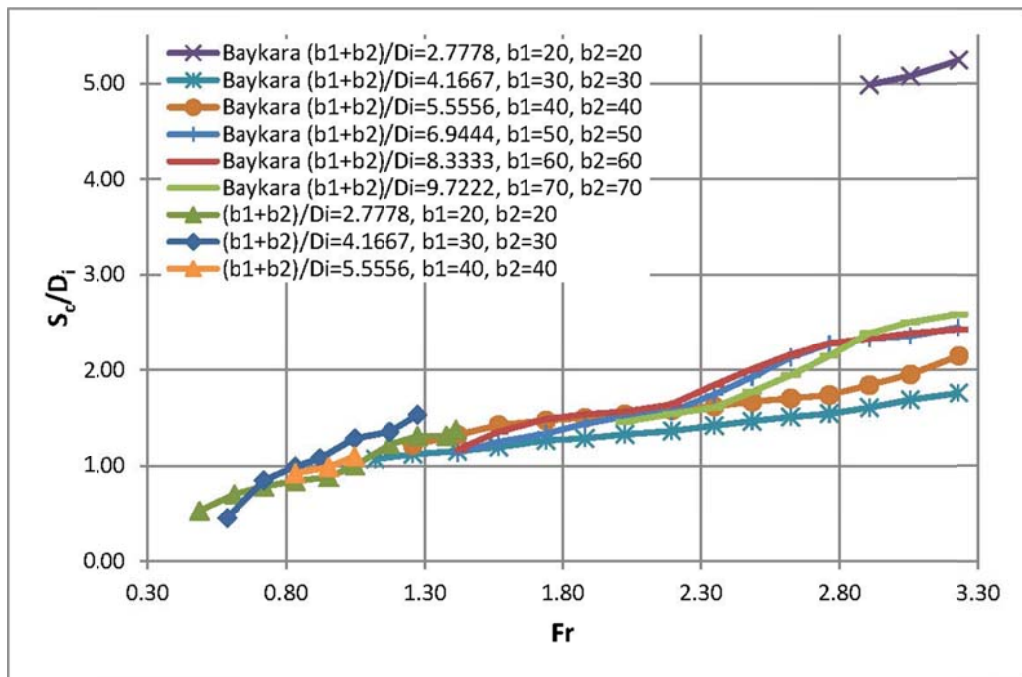
Figure 5.10 Comparison of experiment results of present study with Baykara
2013 S_c/D_i versus Fr as a function of $(b_1+b_2)/D_i$ for D_i=14.4cm
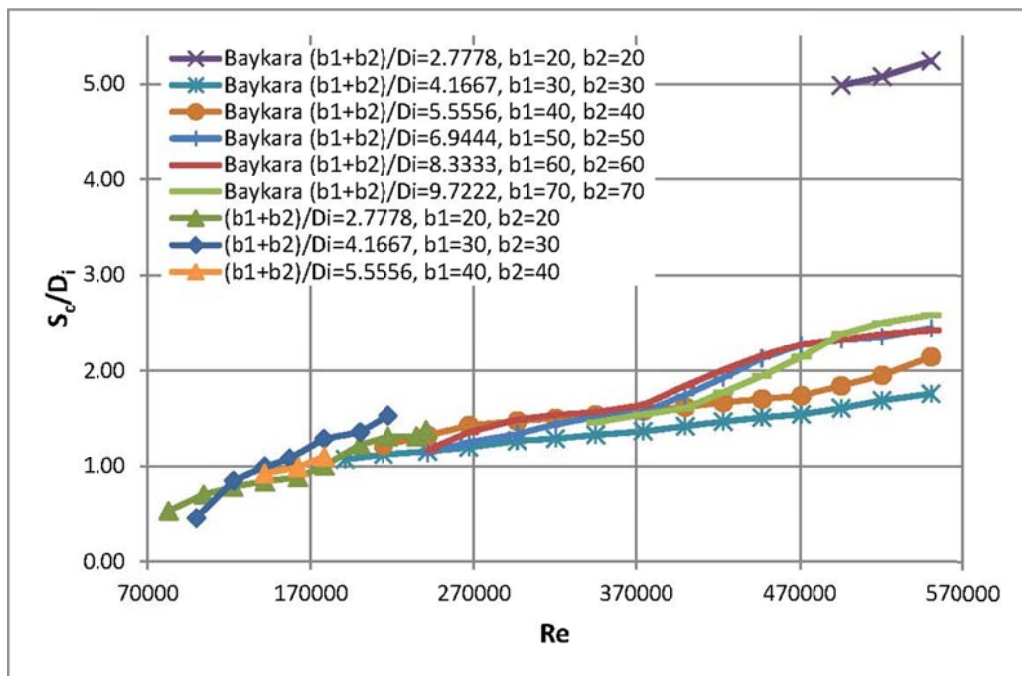
Figure 5.11 Comparison of experiment results of present study with Baykara
2013 S_c/D_i versus Re as a function of $(b_1+b_2)/D_i$ for D_i=14.4cm
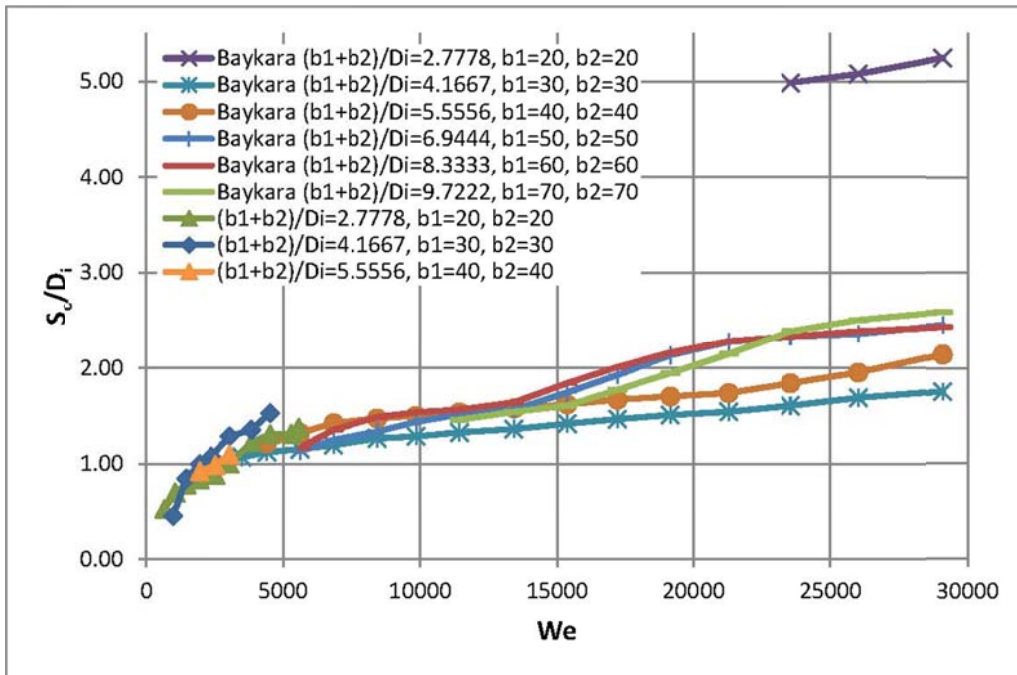
Figure 5.12 Comparison of experiment results of present study with Baykara
2013 S_c/D_i versus We as a function of $(b_1+b_2)/D_i$ for D_i=14.4cm
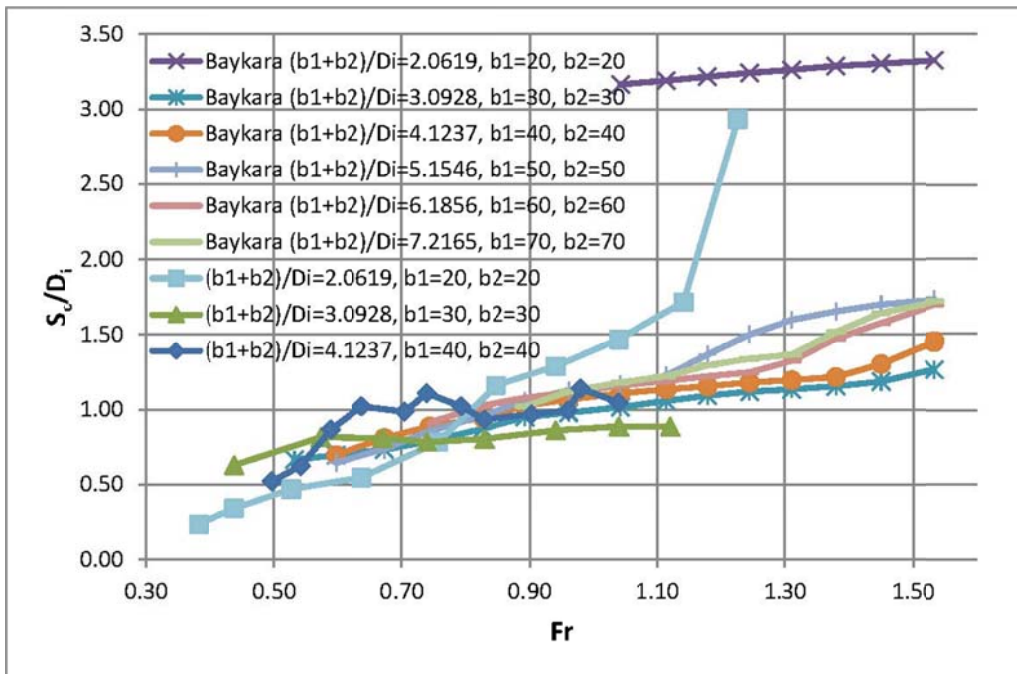
Figure 5.13 Comparison of experiment results of present study with Baykara
2013 S_c/D_i versus Fr as a function of $(b_1+b_2)/D_i$ for D_i=19.4cm
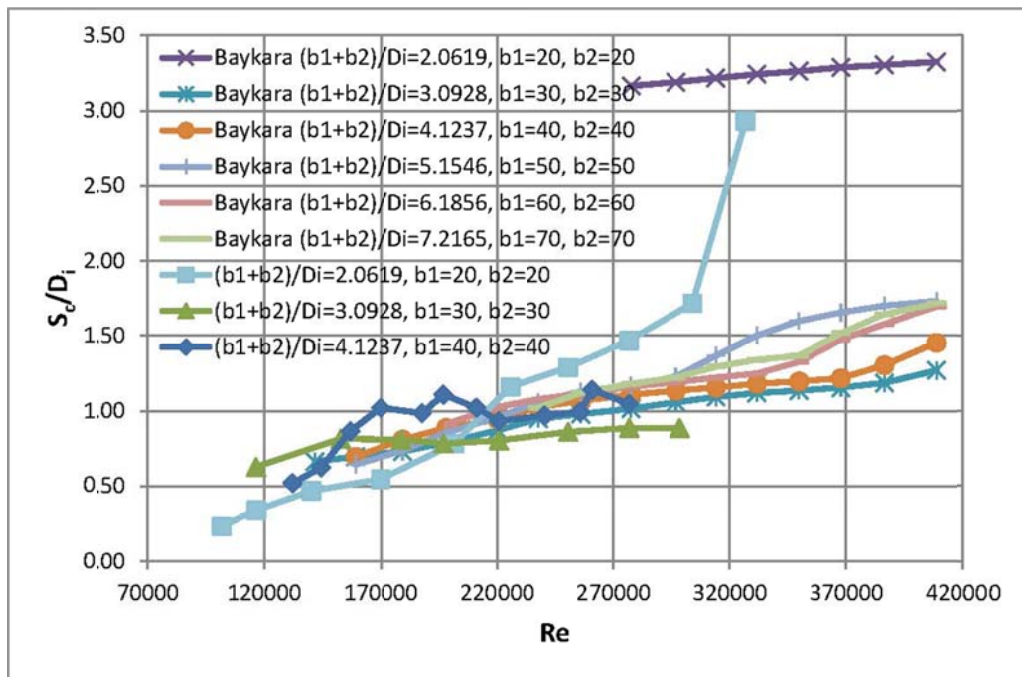
Figure 5.14 Comparison of experiment results of present study with Baykara
2013 S_c/D_i versus Re as a function of $(b_1+b_2)/D_i$ for D_i=19.4cm
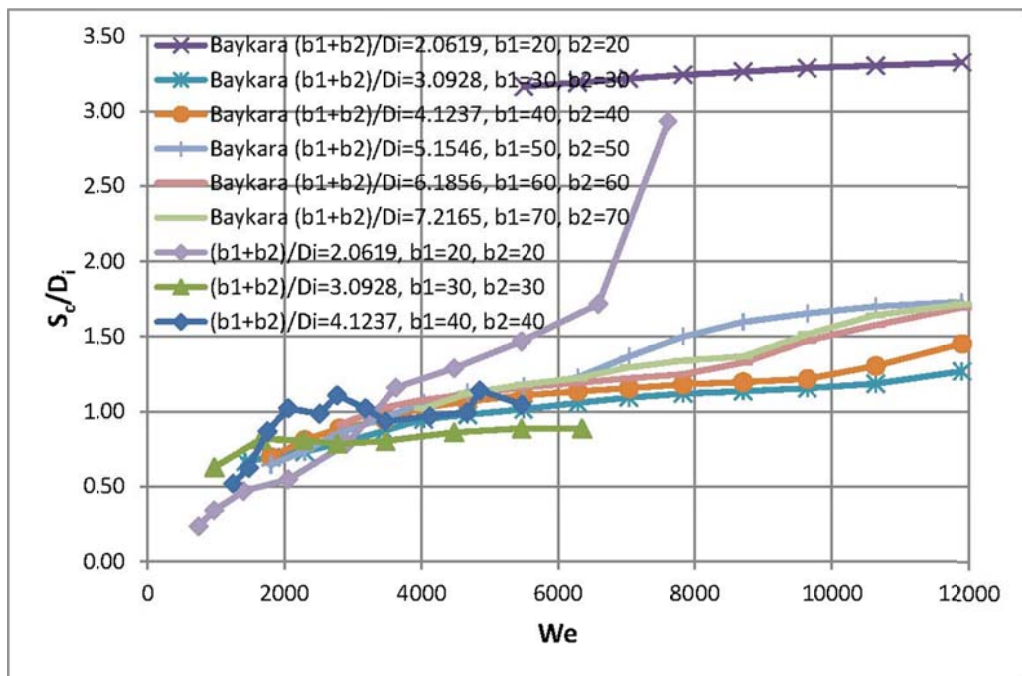
Figure 5.15 Comparison of experiment results of present study with Baykara
2013 S_c/D_i versus We as a function of $(b_1+b_2)/D_i$ for D_i=19.4cm
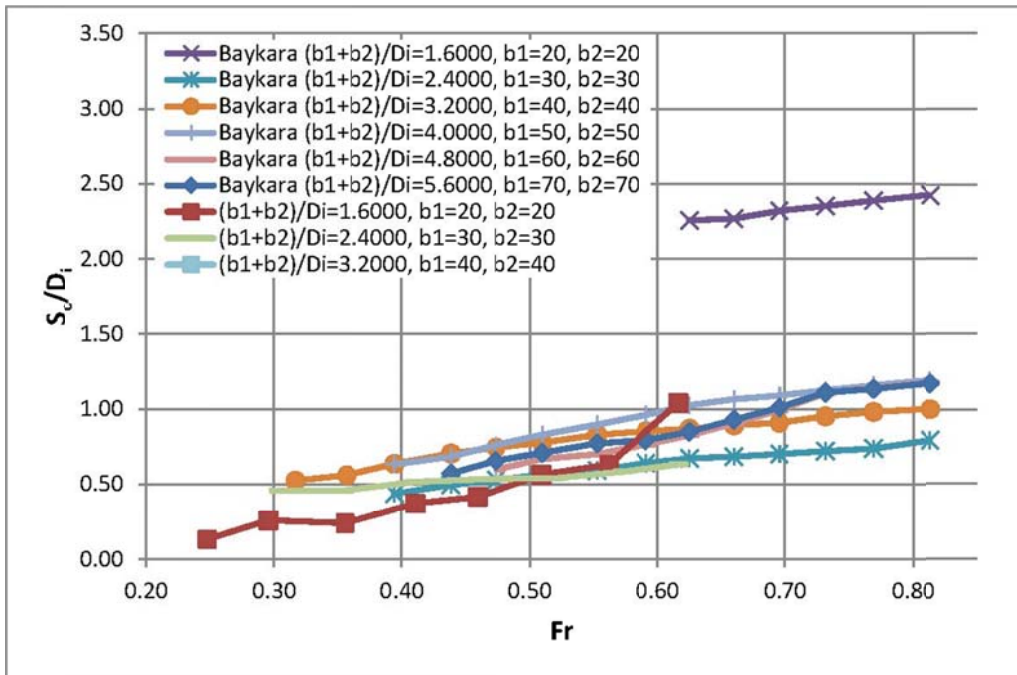
Figure 5.16 Comparison of experiment results of present study with Baykara
2013 S_c/D_i versus Fr as a function of $(b_1+b_2)/D_i$ for D_i=25.0cm
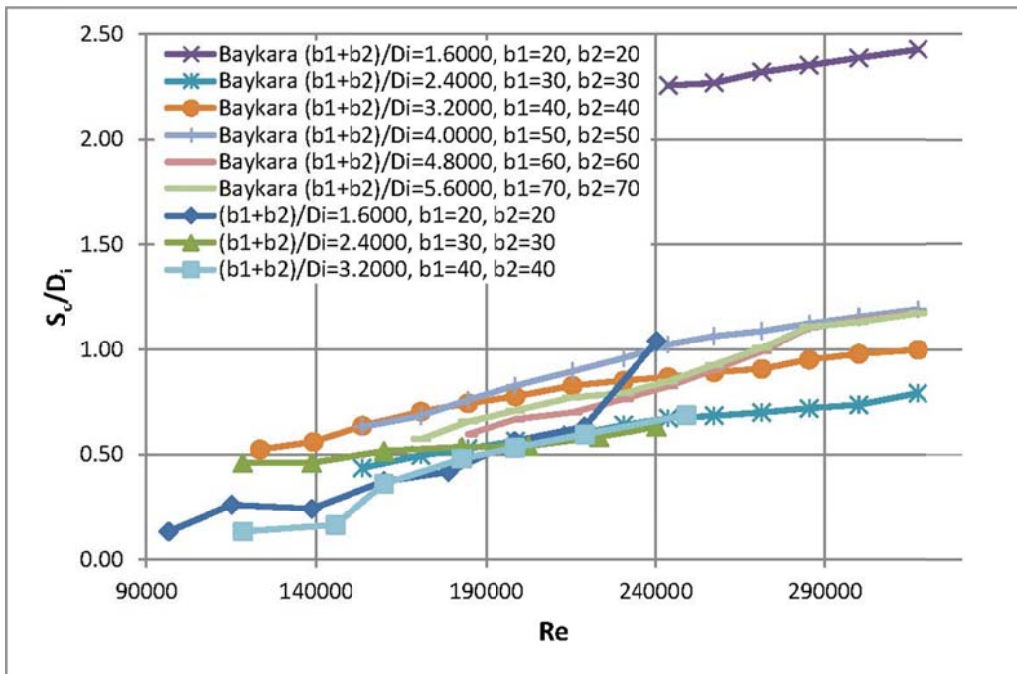
Figure 5.17 Comparison of experiment results of present study with Baykara
2013 S_c/D_i versus Re as a function of $(b_1+b_2)/D_i$ for D_i=25.0cm
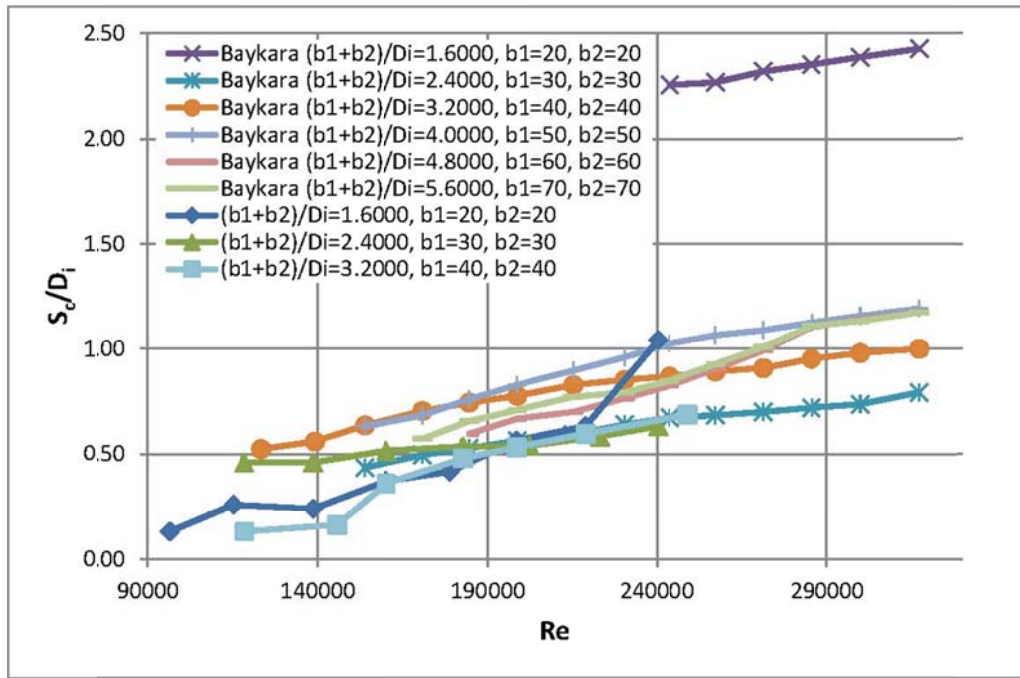
Figure 5.18 Comparison of experiment results of present study with Baykara
2013 S_c/D_i versus We as a function of $(b_1+b_2)/D_i$ for D_i=25.0cm

In general, S_c/D_i values show increasing trend with increasing values of Fr, Re
and We for a given intake diameter.

One important point which can be noticed from the related figures (Figure 5.10
to Figure 5.18) is that for the narrowest side wall clearance; i.e.b_1=b_2=20cm,
S_c/D_i values vary with the related parameters; Fr, Re of We, as the data of the
other $(b_1+b_2)/D_i$ values tested. There is not a clear trend between the curves of
S_c/D_i versus Fr, Re, or We to conclude that how $(b_1+b_2)/D_i$ affect the variation
of S_c/D_i whereas at larger Froude numbers of which the data of S_c/D_i were not
provided such as; $1.30 \leq Fr \leq 2.8$ for D_i=14.4cm, one may say that this zone of
the Froude number is some kind of transition region where S_c/D_i will increase
some how and attain high values at larger values of Fr. At the model of
D_i=19.4cm, the sudden increase of S_c/D_i occurs between the Froude numbers
of about 1.05 and 1.25. Within this zone of Fr for a given Fr, two different
S_c/D_i values are obtained. The similar situation is observed from the data of
D_i=25.0cm where there is a sudden jump in the value of S_c/D_i for the Froude

41

number of about 0.63. In this case there is not a zone of Fr where there are different values of S_c/D_i for a given Fr. From all these assesments it can be stated that only at the narrowest wall clearance; $b_1+b_2=40$cm, at low Froude numbers up to a certain value as a function of intake diameter the variation of S_c/D_i with Fr, Re and We follow a similar trend as the other wall clearances tested. At much larger Froude numbers, S_c/D_i values attain very large values which are not suggested in practical applications. For other wall clearances tested the data of the present study and those of Baykara (2013) are compatible. One can also state that as Fr, Re and We approach to their largest values tested, the rate of change of S_c/D_i with these parameters decreases.

5.2.3. Empirical Equations

5.2.3.1. Application of Regression Analysis to the Present Data

Refering to Equation 3.4 one can write the following equation for the dimensionless critical submergence:

$$\frac{S_c}{D_i} = Fr^{c1}Re^{c2}We^{c3}\left(\frac{(b_1+b_2)}{D_i}\right)^{c4} \qquad\qquad 5.1$$

The gathered symmetrical data from the experiments were used in a multiple variable regression analysis performed by the computer program named DataFit (Oakdale 2012). Consequently, the constants were found as follows.

c1= 0.960

c2= -0.173

c3= 0.271

c4= 0.029

with a correlation coefficient of R^2=0.809

As these coefficients are implemented in Equation 5.1, it takes the following form;

$$\frac{S_c}{D_i} = Fr^{0.960}Re^{-0.173}We^{0.271}\left(\frac{(b_1+b_2)}{D_i}\right)^{0.029} \hspace{3cm} 5.2$$

(valid for the values of Fr, Re, We and (b_1+b_2) /D_i which are within the ranges mentioned in Table 5.1)

In order to demonstrate the correlation of the function given above, the plot of the measured and calculated S_c/D_i values with respect to each other has been shown in Figure 5.19. From this figure and the one which shows the variation of "number of data" with the corresponding "upper limit values of error percentage", Figure 5.20, it can be stated that except for a few data, the calculated values of the related dimensionless parameter stay between $\pm$ 35 % error lines. In these figures units of D_i, b_1 and b_2 are in cm.
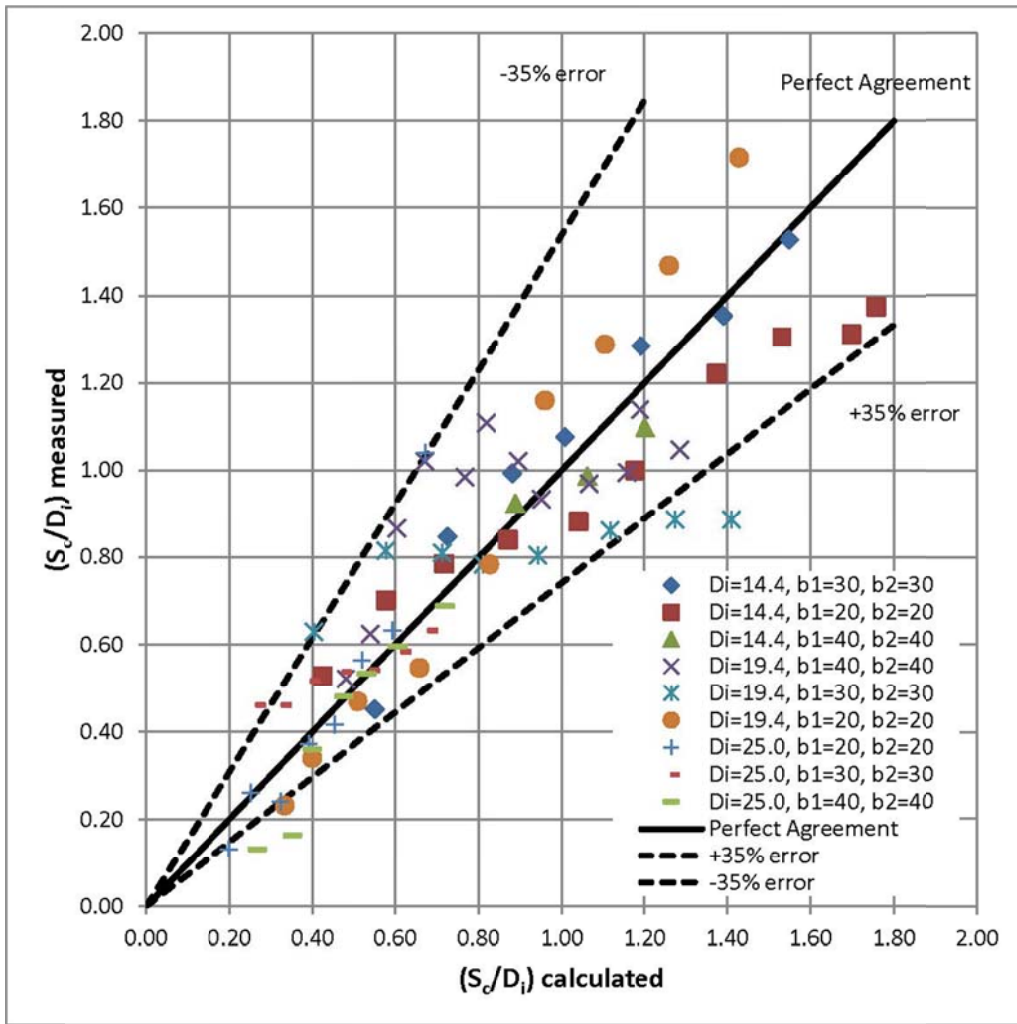
Figure 5.19 Comparison of the measured and calculated S_c/D_i values for the symmetrical lateral wall geometries influenced by all dimensionless parameters mentioned in Equation 5.2
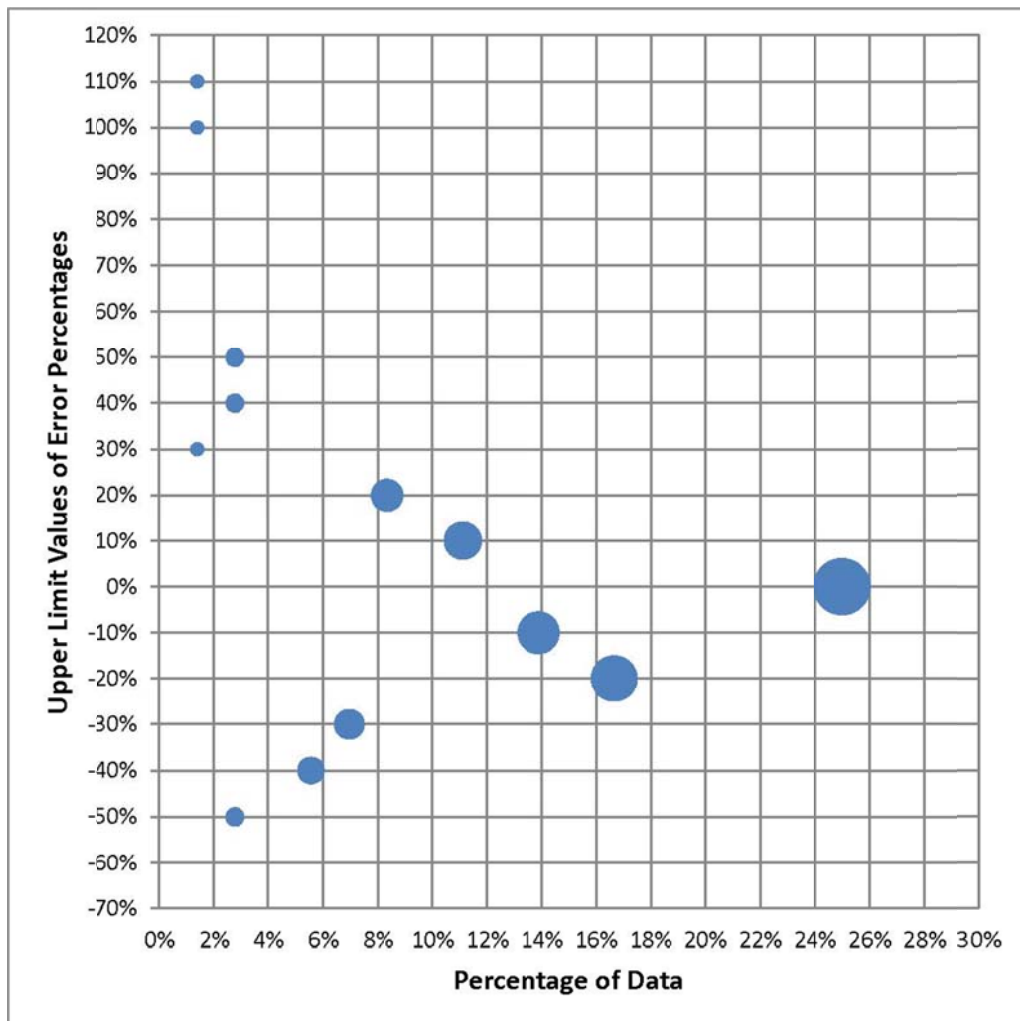
Figure 5.20 Number of data versus upper limit values of error percentages regarding the comparison of the S_c/D_i values calculated by Equation 5.2 and the measurements.

5.2.3.2. Simplification of the Relation of S_c/D_i (Equation 5.2)

If the terms $(b_1{+}b_2)/D_i$, We and Re are omitted from Equation 5.2 one by one to make it simplified and the regression analysis is re-run for each case, the following equations are derived respectively.

$$\frac{S_c}{D_i} = Fr^{0.993}Re^{-0.153}We^{0.247}$$

$\qquad\qquad\qquad\qquad\qquad$ 5.3

with $R^2 = 0.809$

(valid for the values of Fr, Re and We which are within the ranges mentioned in Table 5.1)

$$\frac{S_c}{D_i} = Fr^{1.237}Re^{0.013}$$

$\qquad\qquad\qquad\qquad\qquad$ 5.4

with $R^2 = 0.805$ and

(valid for the values of Fr and Re which are within the ranges mentioned in Table 5.1)

$$\frac{S_c}{D_i} = Fr^{1.057}$$

$\qquad\qquad\qquad\qquad\qquad$ 5.5

with $R^2 = 0.767$.

(valid for the values of Fr between 0.25 to 1.41)

Figure 5.21 to Figure 5.26 show the plot of measured S_c/D_i values with those calculated from the above equations and the variation of "number of data" with the corresponding "upper limit values of error percentages". These figures prevail that as the number of parameters presented in Equation 5.2 is omitted, the error percentages of the related equations slightly changes. In these figures units of D_i, b_1 and b_2 are in cm.
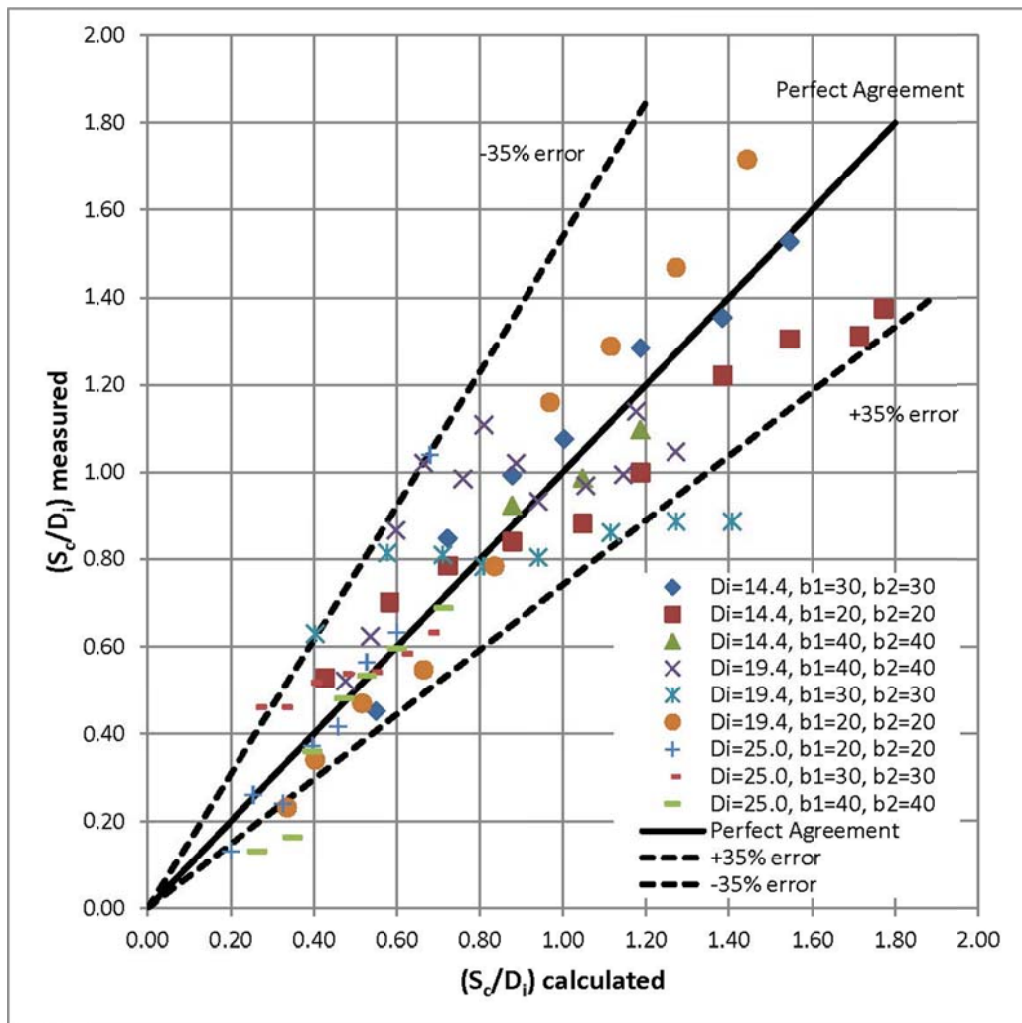
Figure 5.21 Comparison of the measured and calculated S_c/D_i values under influence of the dimensionless parameters mentioned in Equation 5.3
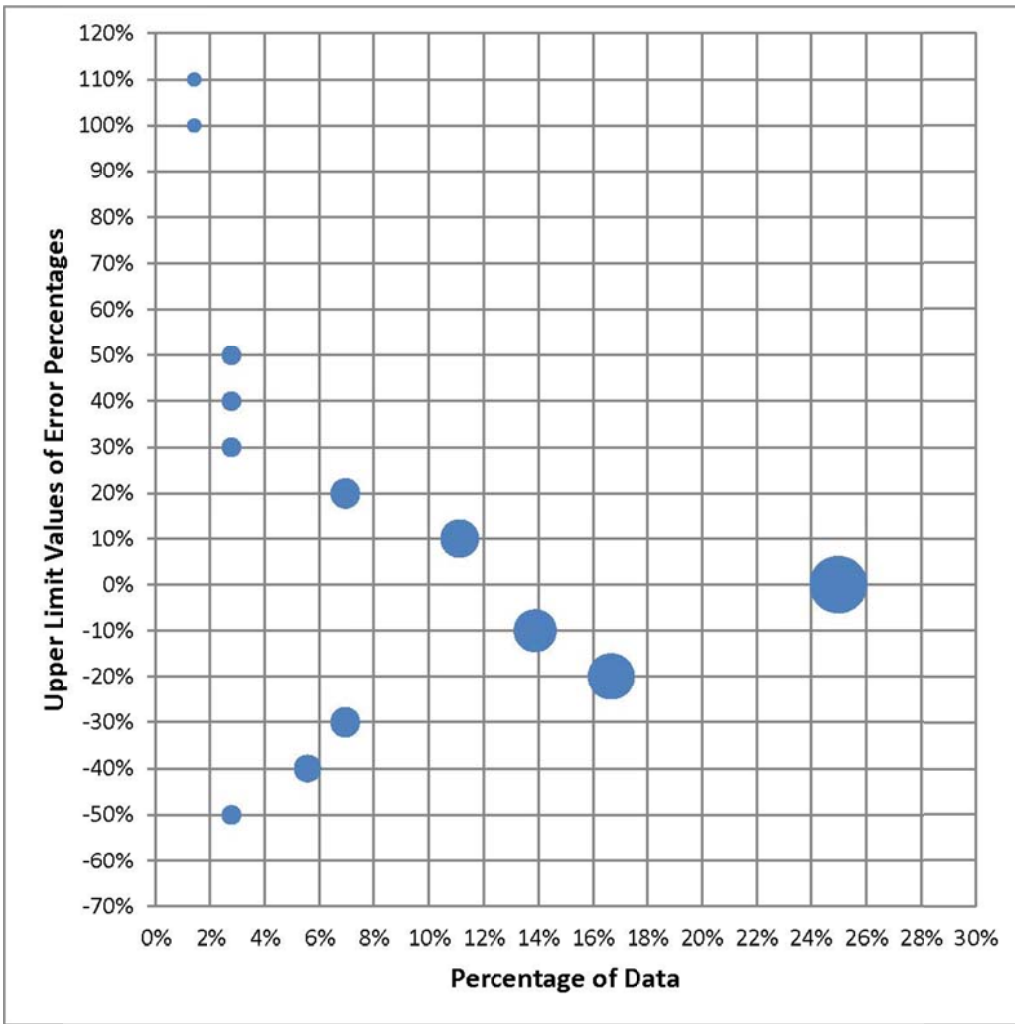
Figure 5.22 Number of data versus upper limit values of error percentages regarding the comparison of the S_c/D_i values calculated by Equation 5.3 and the measurements.
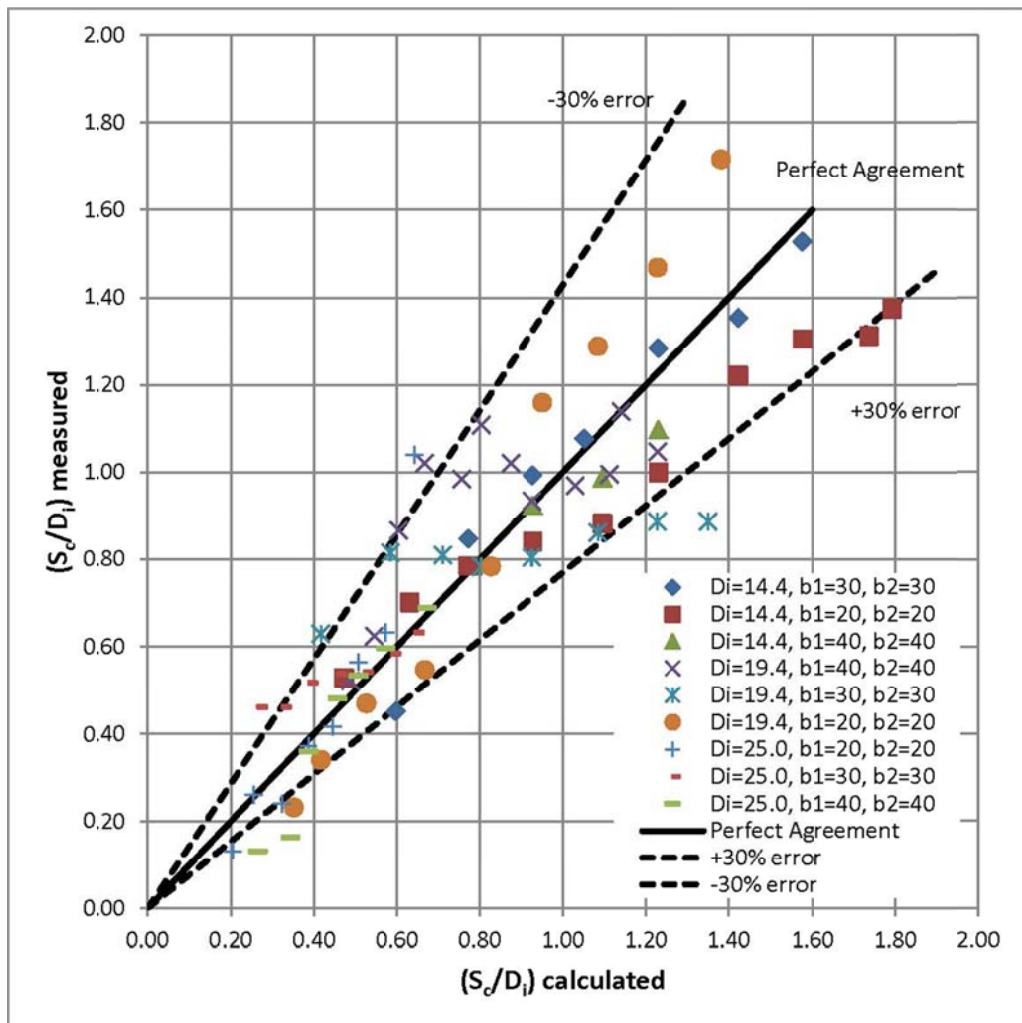
Figure 5.23 Comparison of the measured and calculated S_c/D_i values under influence of the dimensionless parameters mentioned in Equation 5.4
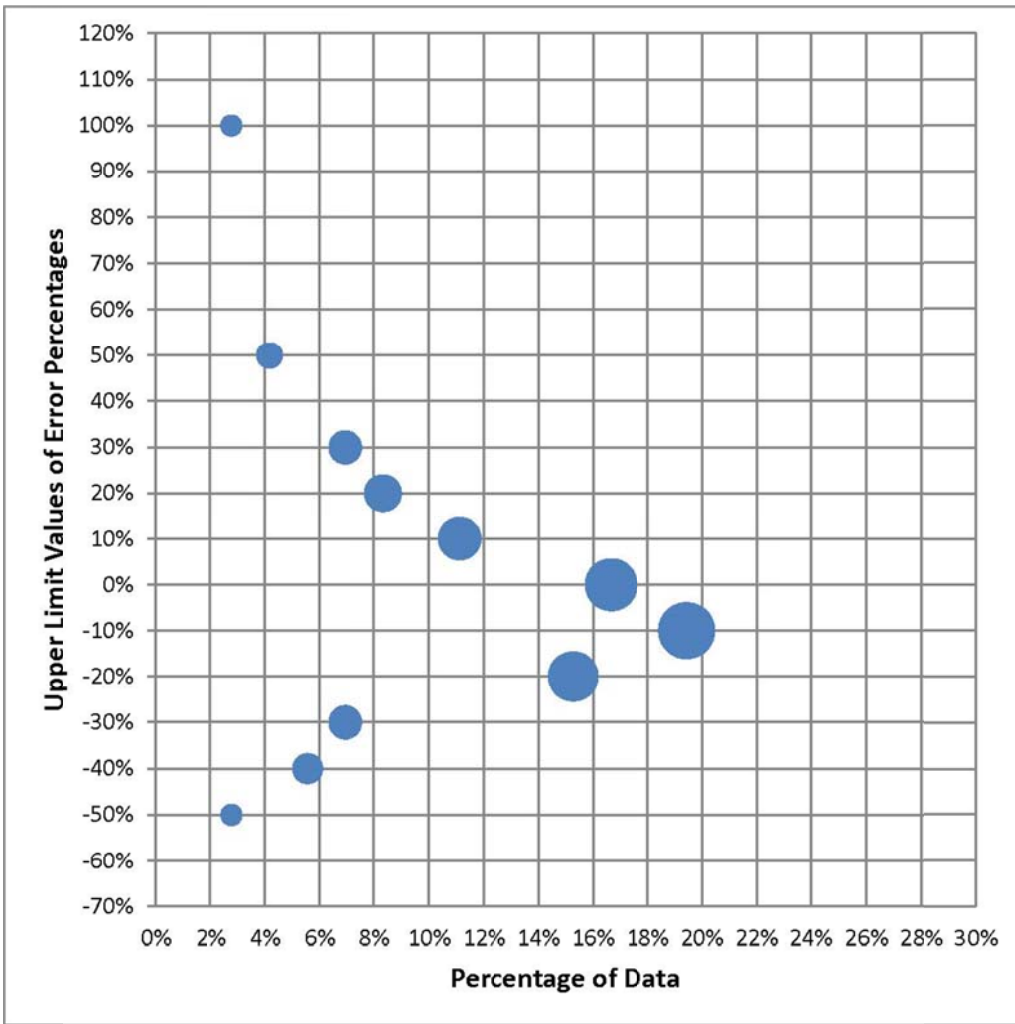
Figure 5.24 Number of data versus upper limit values of error percentages regarding the comparison of the S_c/D_i values calculated by Equation 5.4 and the measurements.
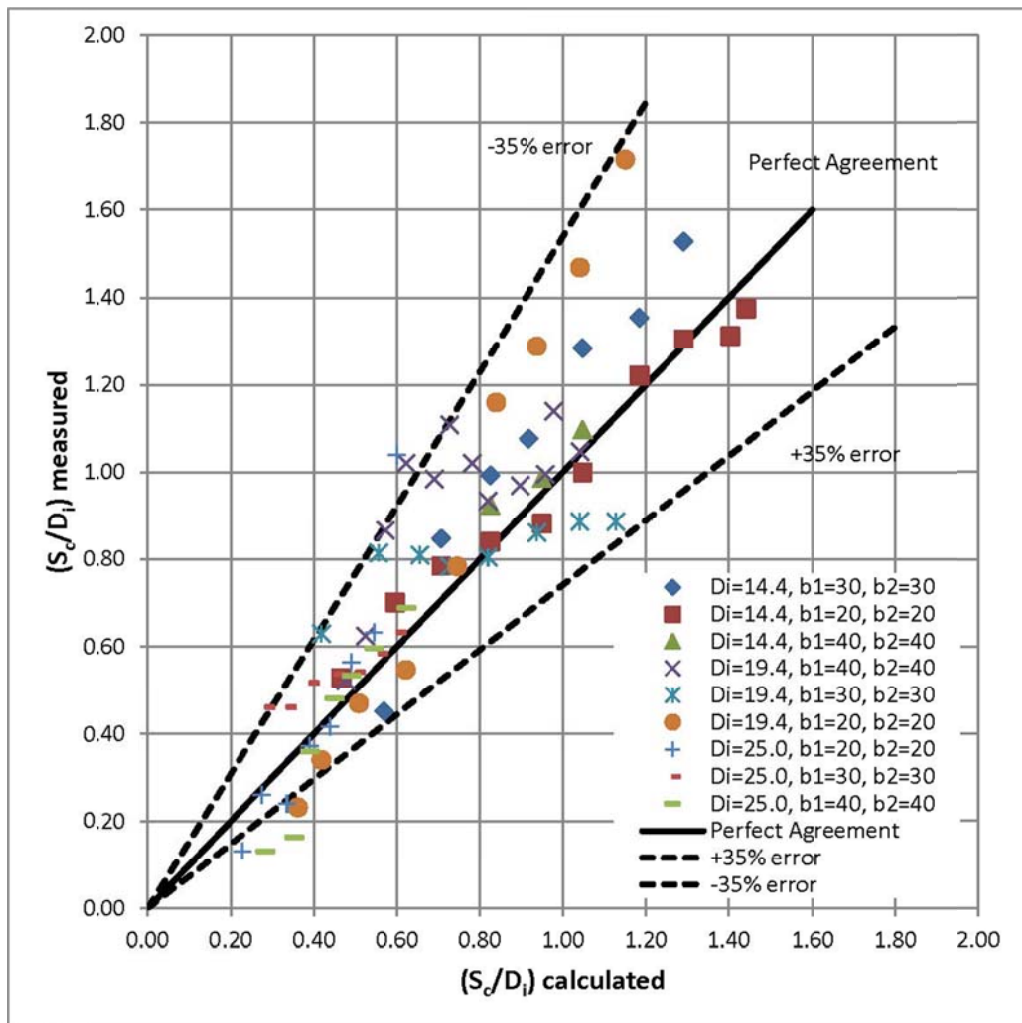
Figure 5.25 Comparison of the measured and calculated S_c/D_i values under influence of the dimensionless parameters mentioned in Equation 5.5
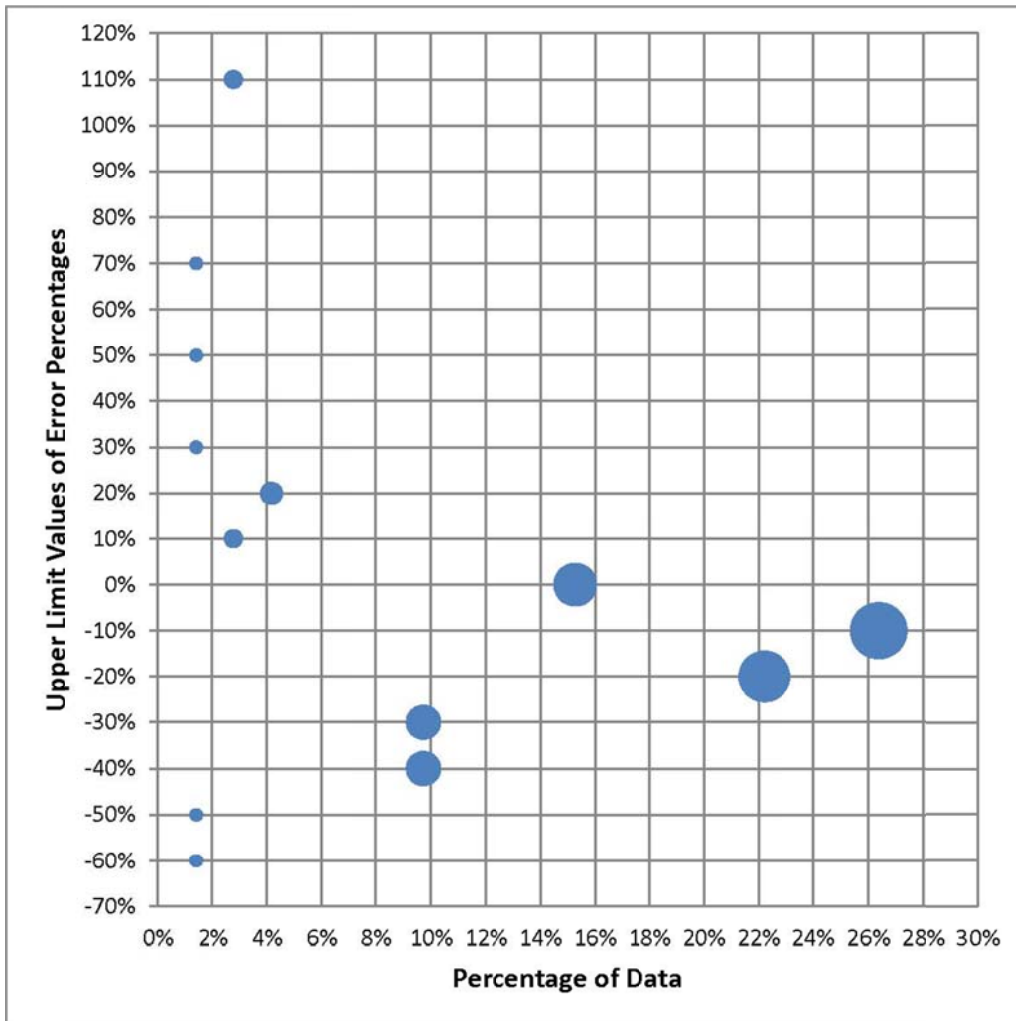
Figure 5.26 Number of data versus upper limit values of error percentages regarding the comparison of the S_c/D_i values calculated by Equation 5.5 and the measurements.

5.3. ASYMMETRICAL SIDE WALL CLEARANCES

5.3.1. Effect of Dimensionless Parameters on S_c/D_i

The plotted relations of the dimensionless parameters according to the experimental results are presented between Figure 5.27 and Figure 5.35. In these figures units of b_1 and b_2 are in cm.
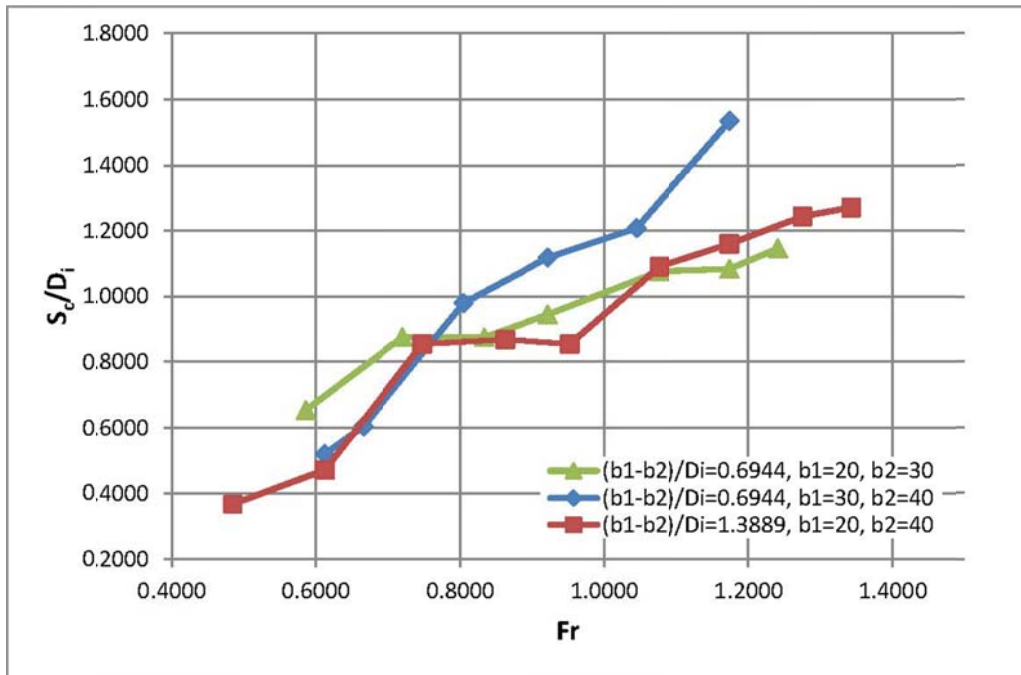
Figure 5.27 S_c/D_i versus Fr as a function of $|(b_1-b_2)|/D_i$ for D_i=14.4cm
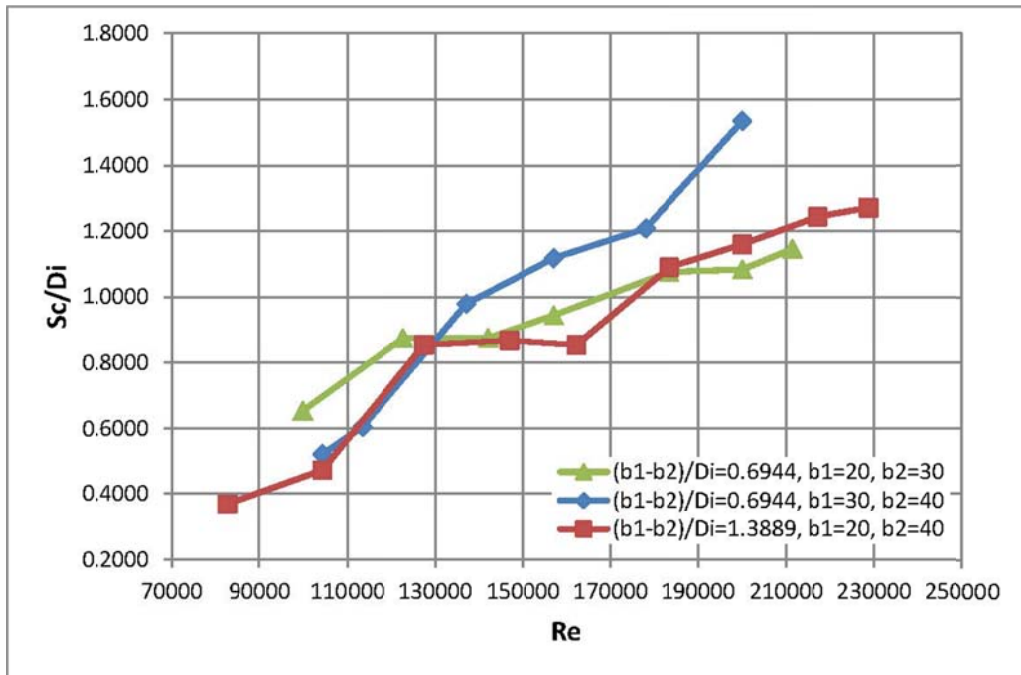
Figure 5.28 S_c/D_i versus Re as a function of $|(b_1-b_2)|/D_i$ for D_i=14.4cm
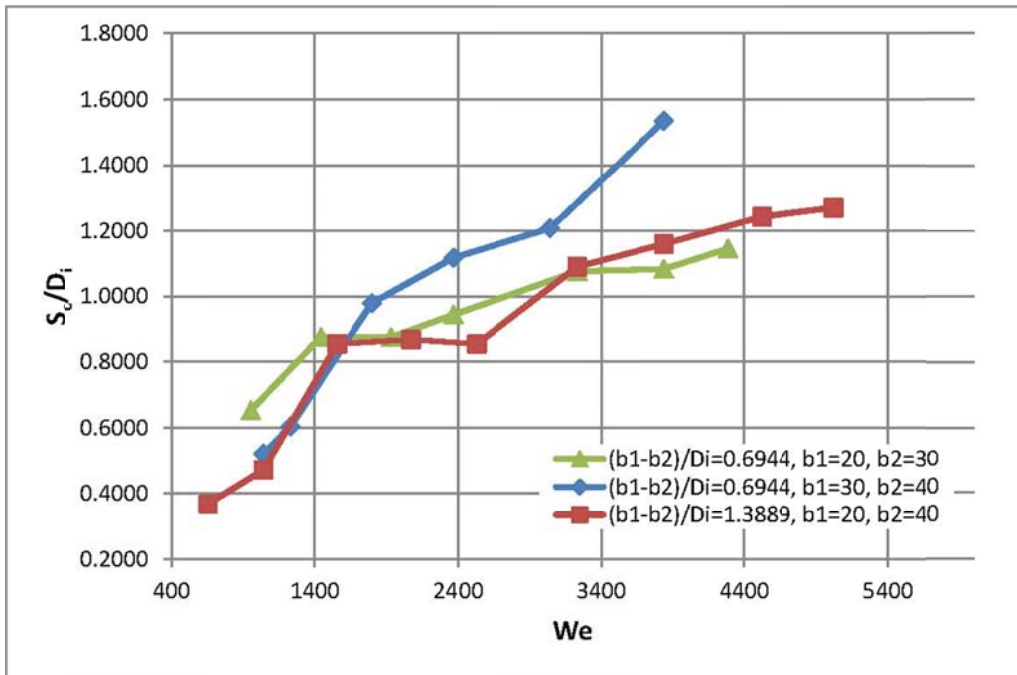
Figure 5.29 S_c/D_i versus We as a function of $|(b_1-b_2)|/D_i$ for D_i=14.4cm
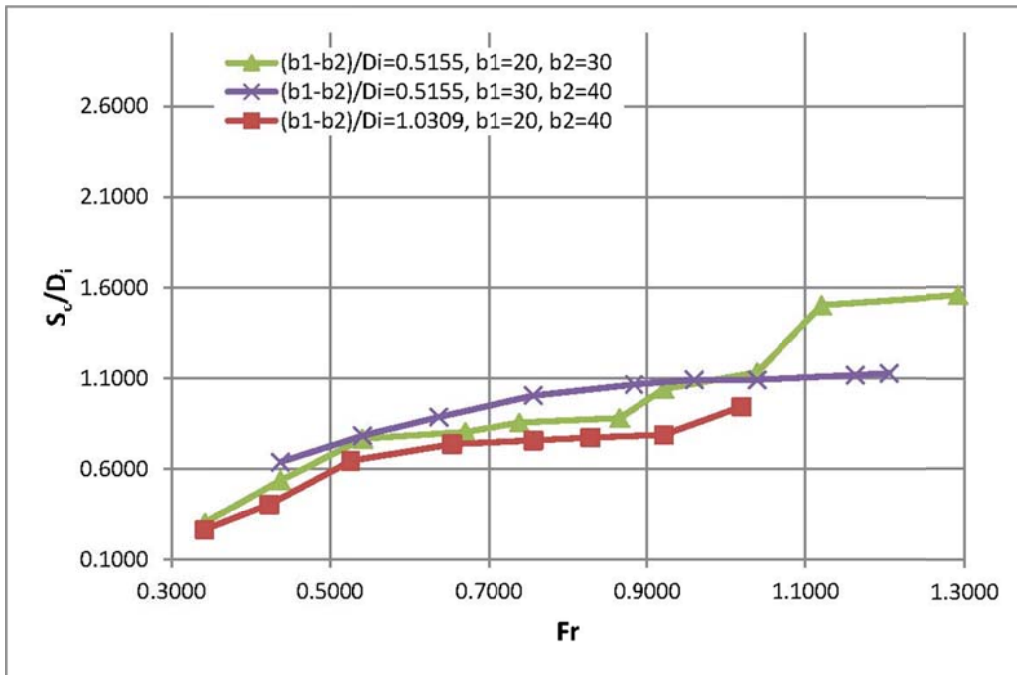
Figure 5.30 S_c/D_i versus Fr as a function of $|(b_1-b_2)|/D_i$ for D_i=19.4cm
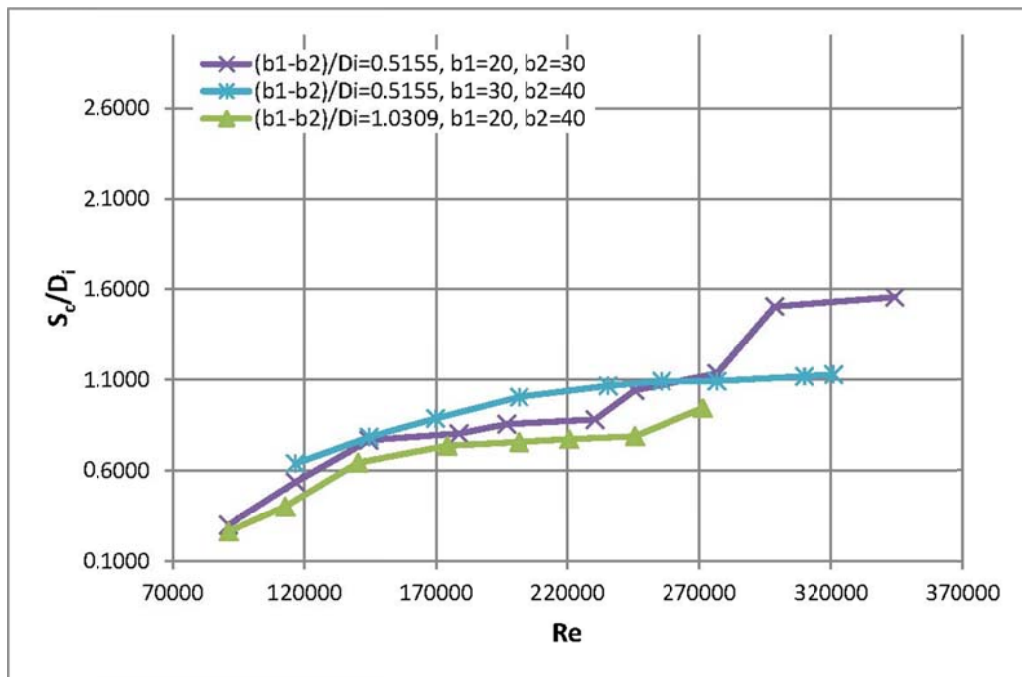
Figure 5.31 S_c/D_i versus Re as a function of $|(b_1-b_2)|/D_i$ for D_i=19.4cm
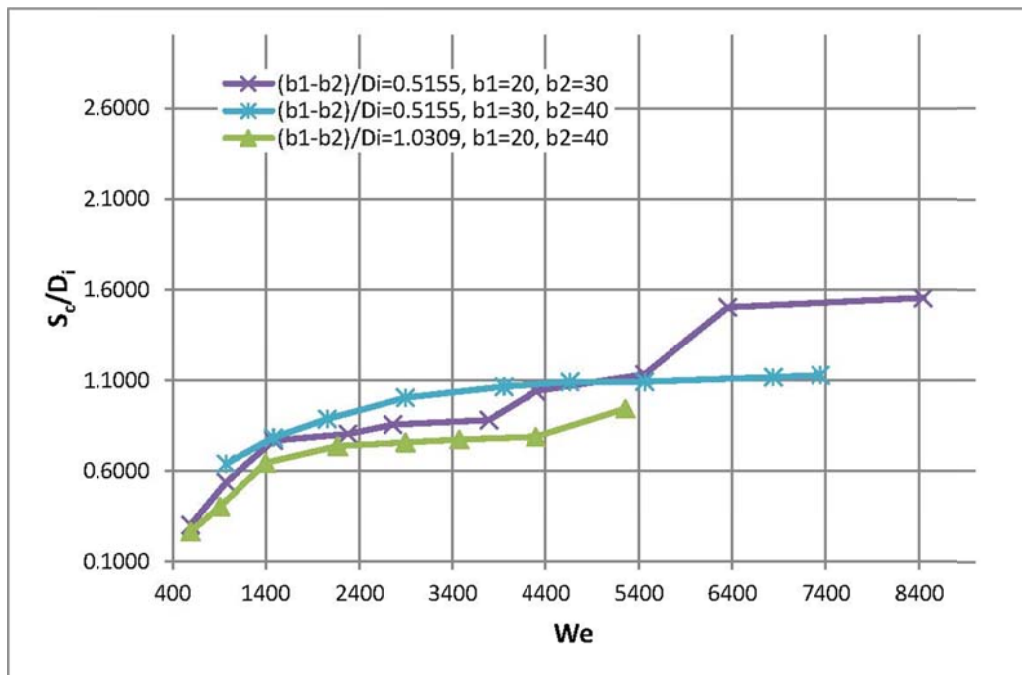
Figure 5.32 S_c/D_i versus We as a function of $|(b_1-b_2)|/D_i$ for D_i=19.4cm
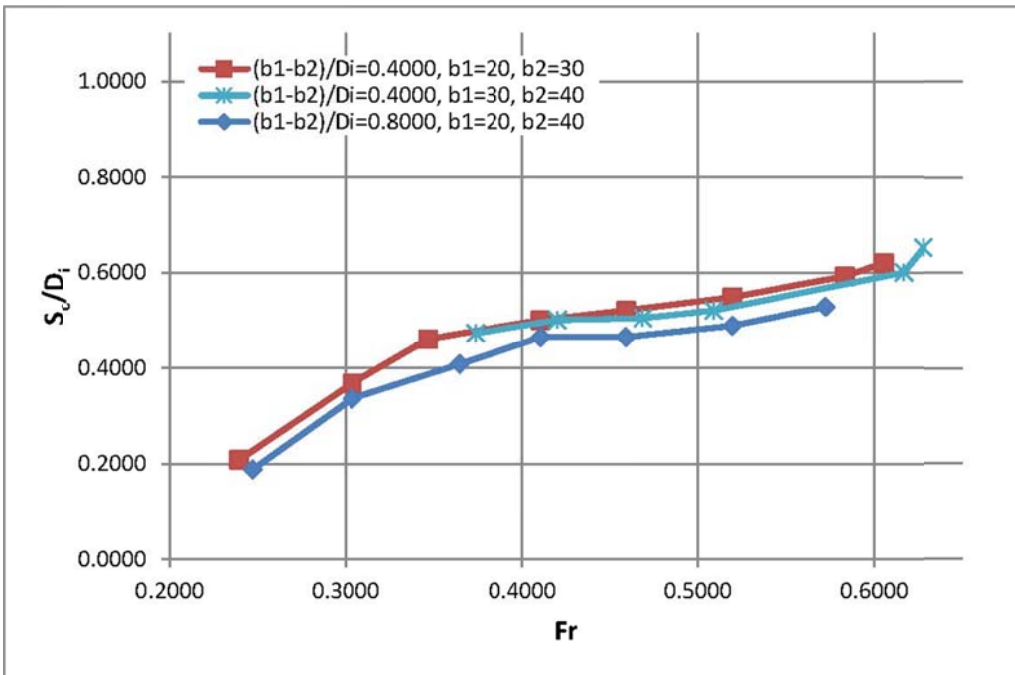
Figure 5.33 S_c/D_i versus Fr as a function of $|(b_1-b_2)|/D_i$ for $D_i=25.0$cm
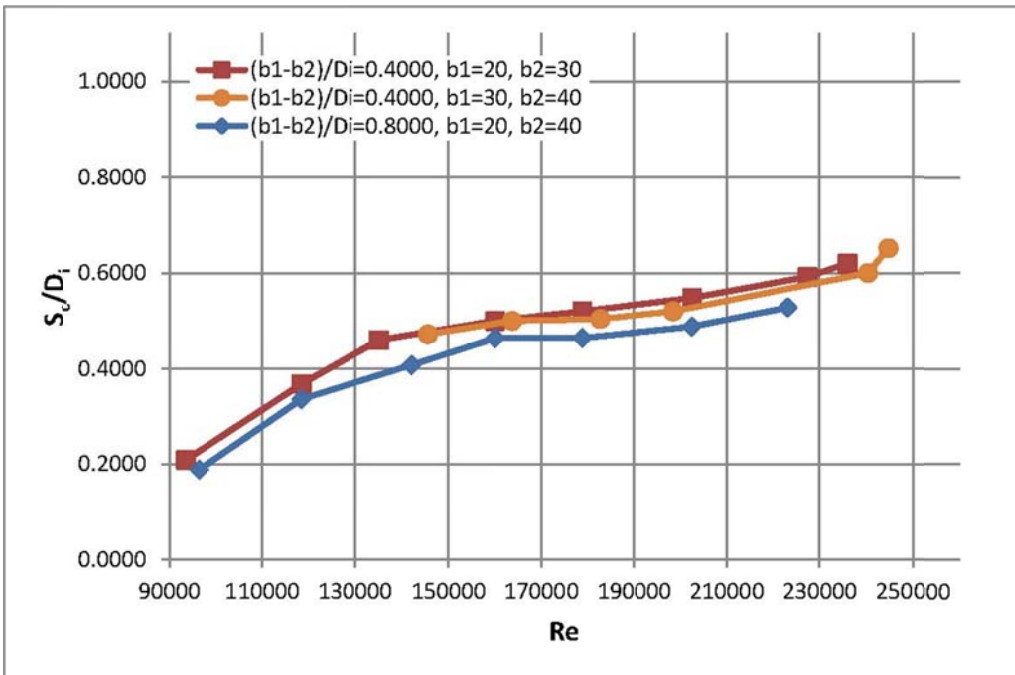
Figure 5.34 S_c/D_i versus Re as a function of $|(b_1-b_2)|/D_i$ for $D_i=25.0$cm
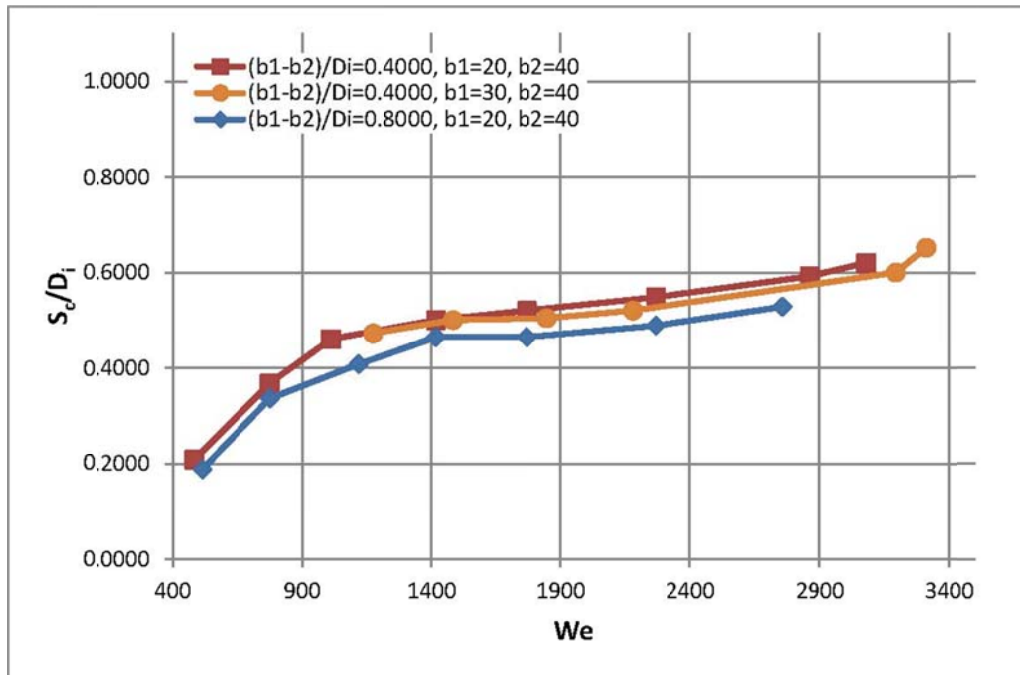
Figure 5.35 S_c/D_i versus We as a function of $|(b_1-b_2)|/D_i$ for $D_i=25.0$ cm

These figures can be evaluated as follows:

S_c/D_i values show increasing trend with increasing values of Fr, Re and We for a given intake diameter. Within the limits of the parameters Fr, Re and We tested one can not give limit values for these parameters beyond which S_c/D_i is independent of them. It is difficult to state something about the effect of $|(b_1-b_2)|/D_i$ on the variation of S_c/D_i since the curves of S_c/D_i versus Fr, Re and We intersect each other at various points on the related figures. Therefore, the relations between these parameters are to be presented in the forms of empirical equations in the following sections.

5.3.2. Empirical Equations

5.3.2.1. Application of Regression Analysis to the Present Data

A relationship for the dimensionless critical submergence can be stated by considering Equation 3.5 as follows:

$$\frac{S_c}{D_i} = Fr^{c1}Re^{c2}We^{c3}\left(\frac{|(b_1-b_2|)}{D_i}\right)^{c4} \qquad 5.6$$

The data of S_c/D_i and related dimensionless parameters obtained from the experiments conducted with asymmetrical side walls were used in a multiple variable regression analysis performed by the computer program named DataFit (Oakdale 2012). Consequently, the constants given in Equation 5.6 were found as follows.

c1= 1.162

c2= 0.069

c3= -0.103

c4= -0.210

with a correlation coefficient of $R^2 = 0.914$

As these coefficients are substituted in Equation 5.6, it takes the following form;

$$\frac{S_c}{D_i} = Fr^{1.162}Re^{0.069}We^{-0.103}\left(\frac{|(b_1-b_2)|}{D_i}\right)^{-0.210} \qquad 5.7$$

(valid for the values of Fr, Re, We and $|(b_1-b_2)|/D_i$ which are within the ranges mentioned in Table 5.2)

In order to demonstrate the correlation of the function, the plot of the measured and calculated S_c/D_i values with respect to each other has been shown in Figure 5.36. From this figure and the one which shows the variation of "number of data" with the corresponding "upper limit values of error percentages", Figure 5.37, it can be concluded that except just a few data, the calculated S_c/D_i values stay between ± 25 % error lines. In these figures units of D_i, b_1 and b_2 are in cm.
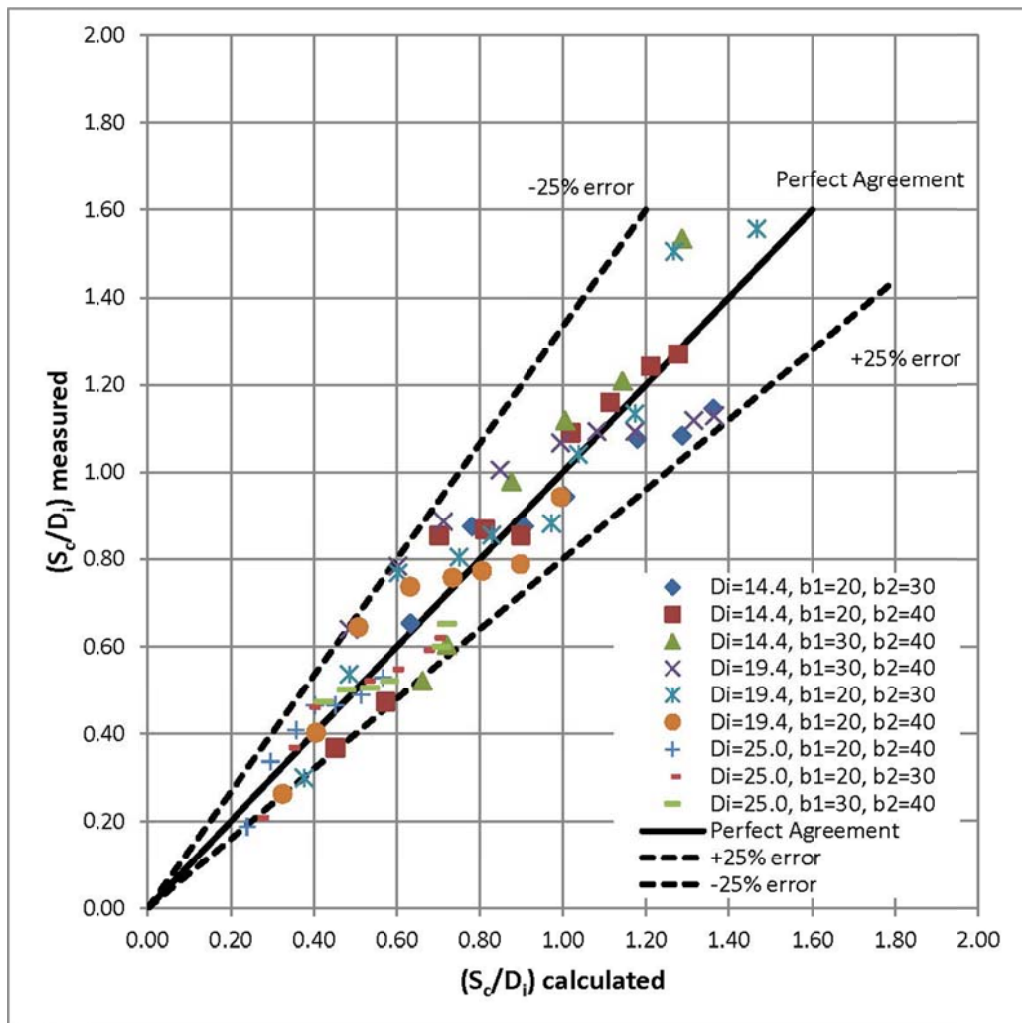
Figure 5.36 Comparison of the measured and calculated S_c/D_i values for the asymmetrical lateral wall geometries influenced by all dimensionless parameters mentioned in Equation 5.7
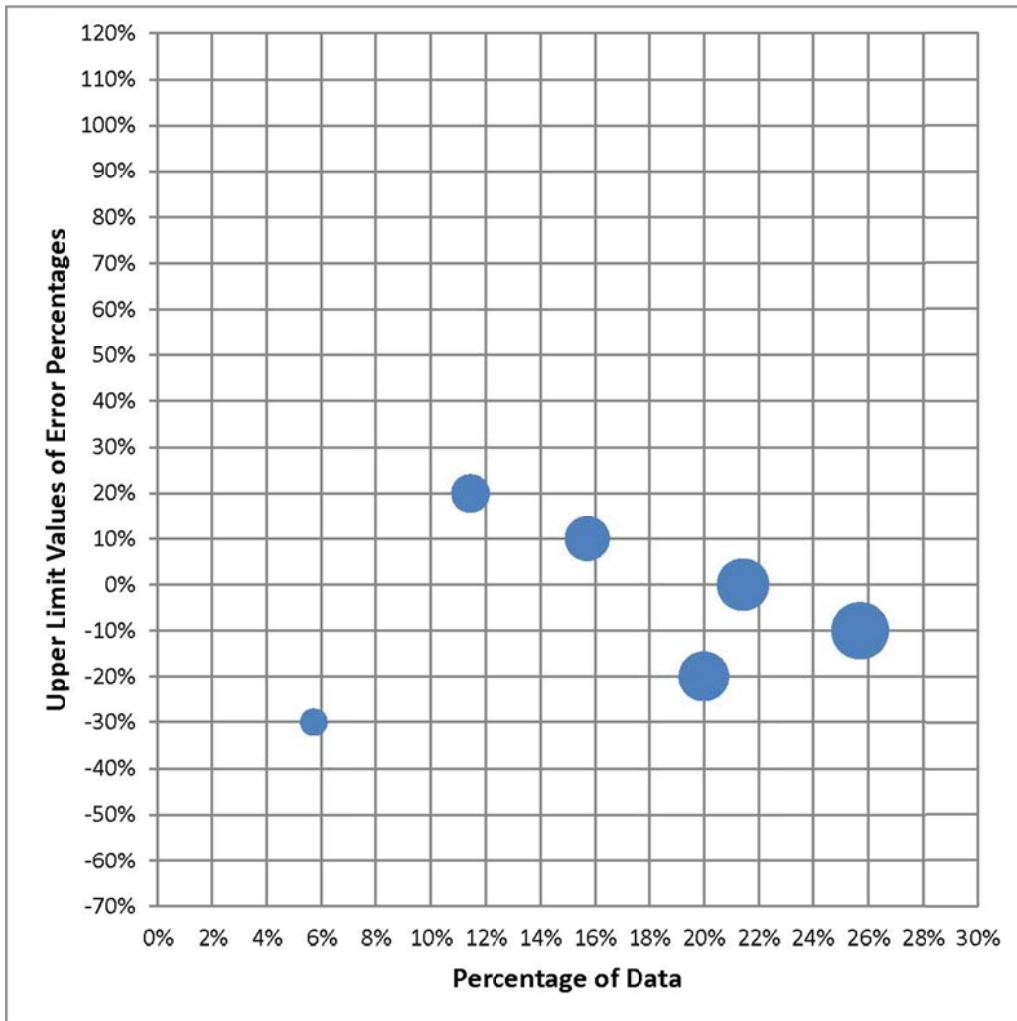
Figure 5.37 Number of data versus upper limit values of error percentages
regarding the comparison of the S_c/D_i values calculated by Equation 5.7 and
the measurements.

5.3.2.2. Simplification of the Relation of S_c/D_i (Equation 5.7)

If the terms $|(b_1-b_2)|/D_i$, We and Re are ommited from Equation 5.7 one by one
and the regression analysis is re-run for each case, the following equations are
derived respectively.

60

$$\frac{S_c}{D_i} = Fr^{0.835} Re^{-0.104} We^{0.162}$$ 5.8

with $R^2 = 0.892$ for the case.

(valid for the values of Fr, Re and We which are within the ranges mentioned in Table 5.2)

$$\frac{S_c}{D_i} = Fr^{0.999} Re^{0.005}$$ 5.9

with $R^2 = 0.889$ for the case.

(valid for the values of Fr and Re which are within the ranges mentioned in Table 5.2)

$$\frac{S_c}{D_i} = Fr^{0.933}$$ 5.10

with $R^2 = 0.880$ for the case.

(valid for the values of Fr between 0.24 to 1.34)

Figure 5.38 to Figure 5.43 show the plot of measured S_c/D_i values with those calculated from above equations and the variation of "number of data" with the coresponding "upper limit of error percentages". These figures prevail that as the number of the parameters to be omitted from Equation 5.7 is increased, the error percentages of the related equations do not change. In these figures units of D_i, b_1 and b_2 are in cm.
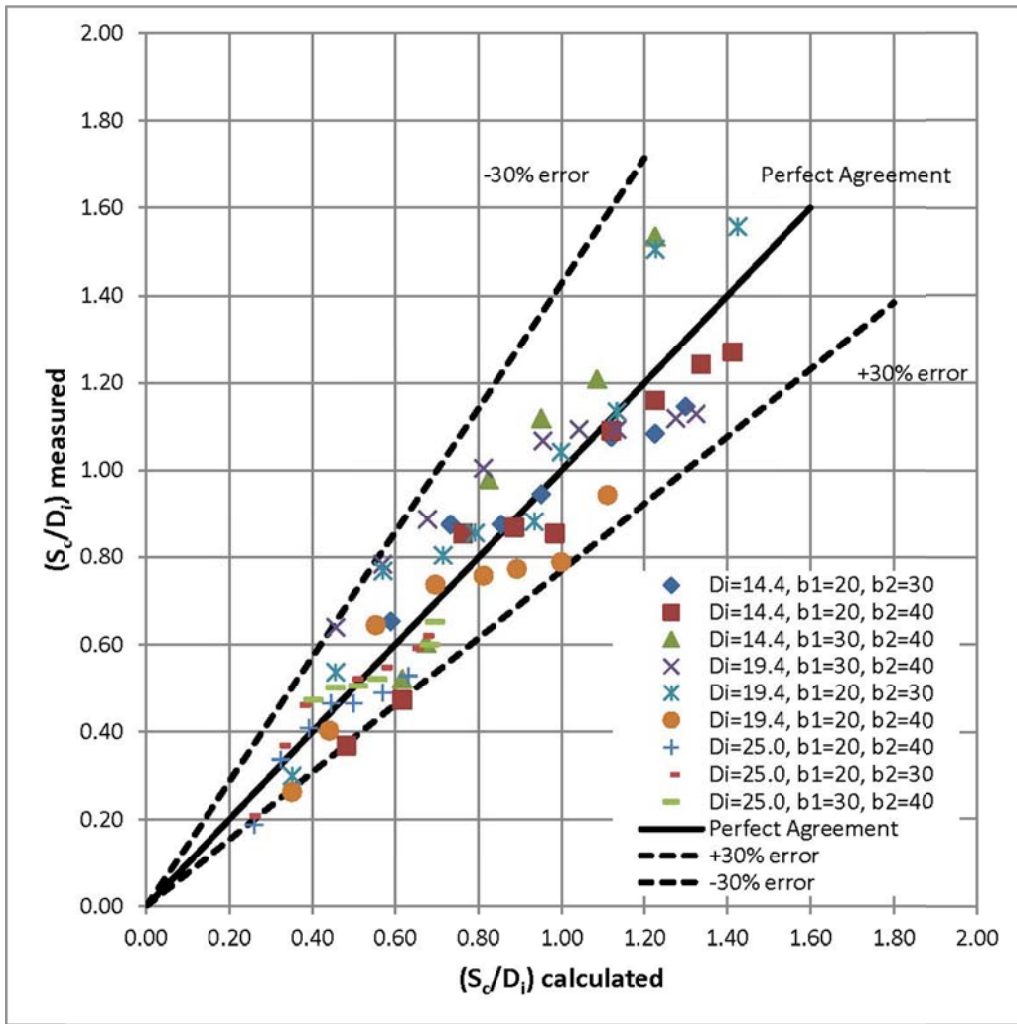
Figure 5.38 Comparison of the measured and calculated S_c/D_i values under influence of the dimensionless parameters mentioned in Equation 5.8
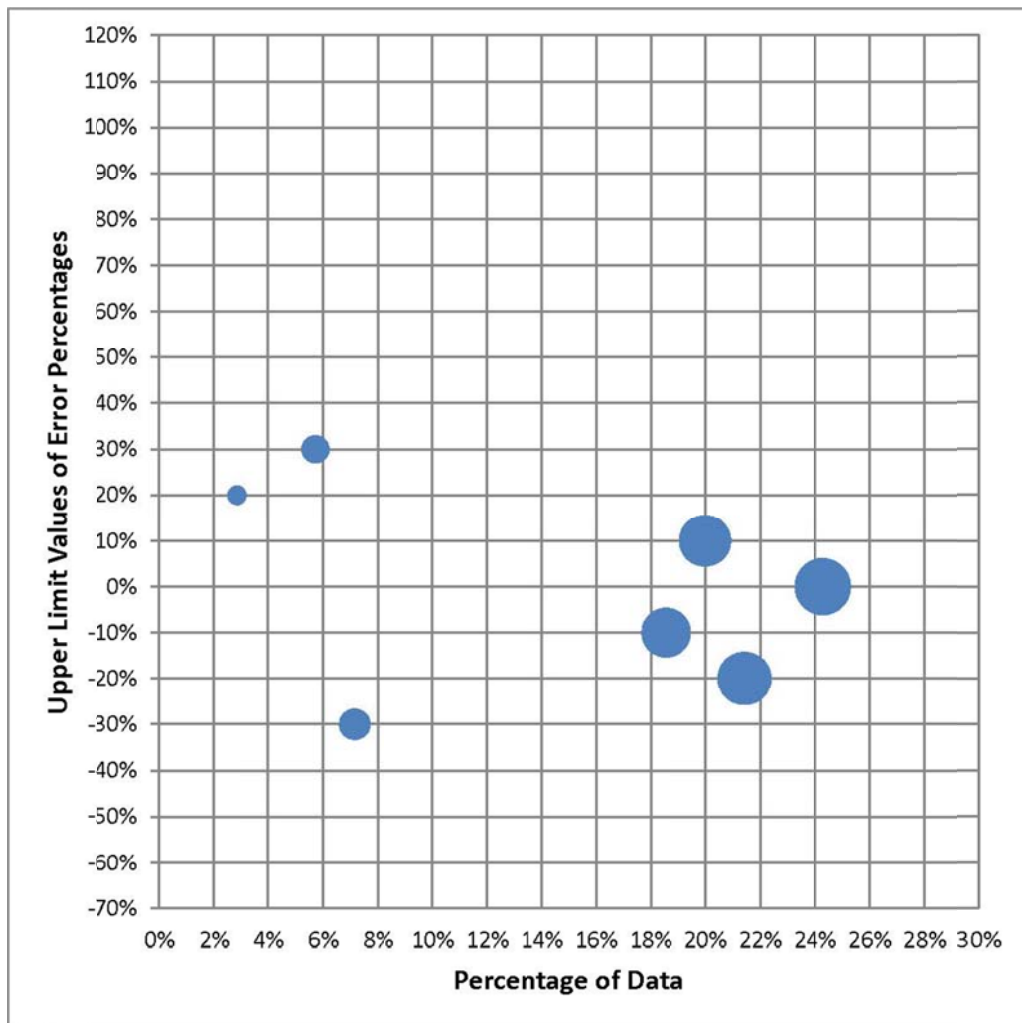
Figure 5.39 Number of data versus upper limit values of error percentages regarding the comparison of the S_c/D_i values calculated by Equation 5.8 and the measurements.
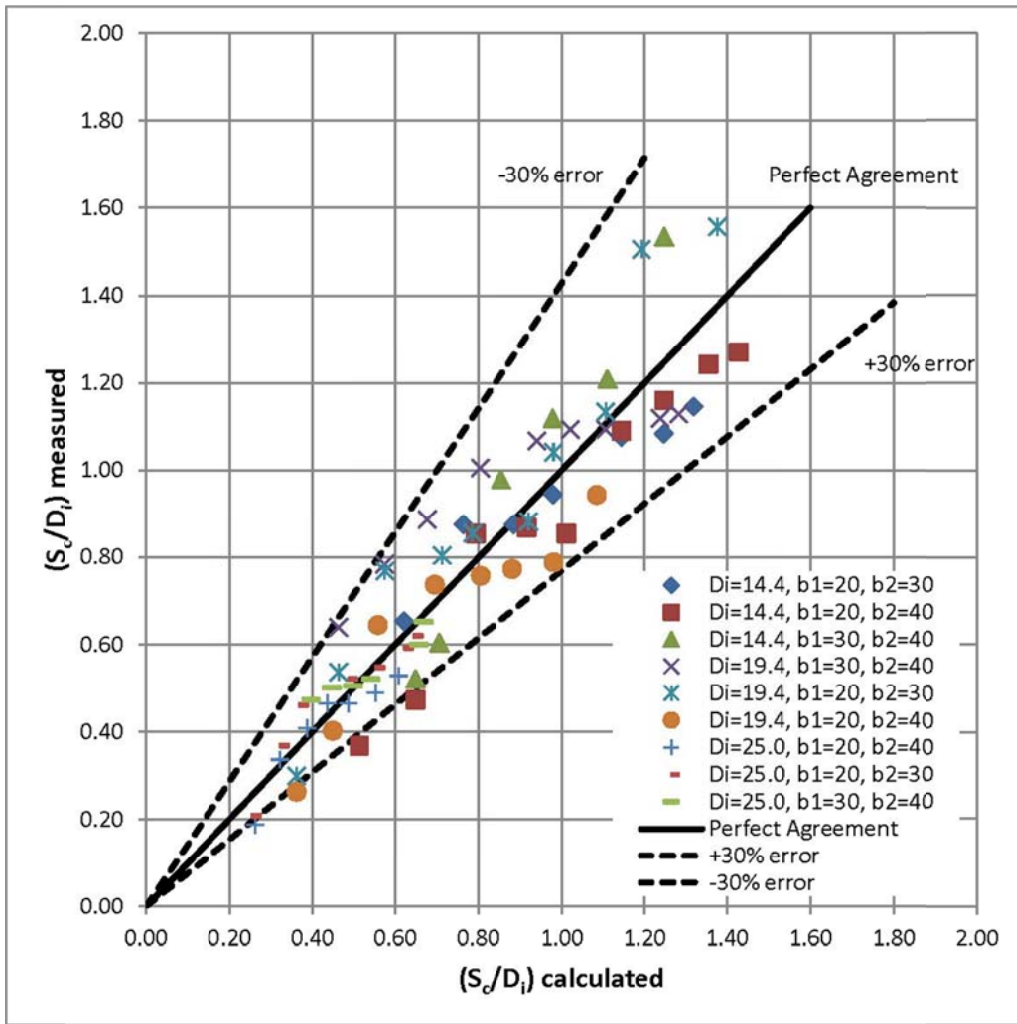
Figure 5.40 Comparison of the measured and calculated S_c/D_i values under influence of the dimensionless parameters mentioned in Equation 5.9
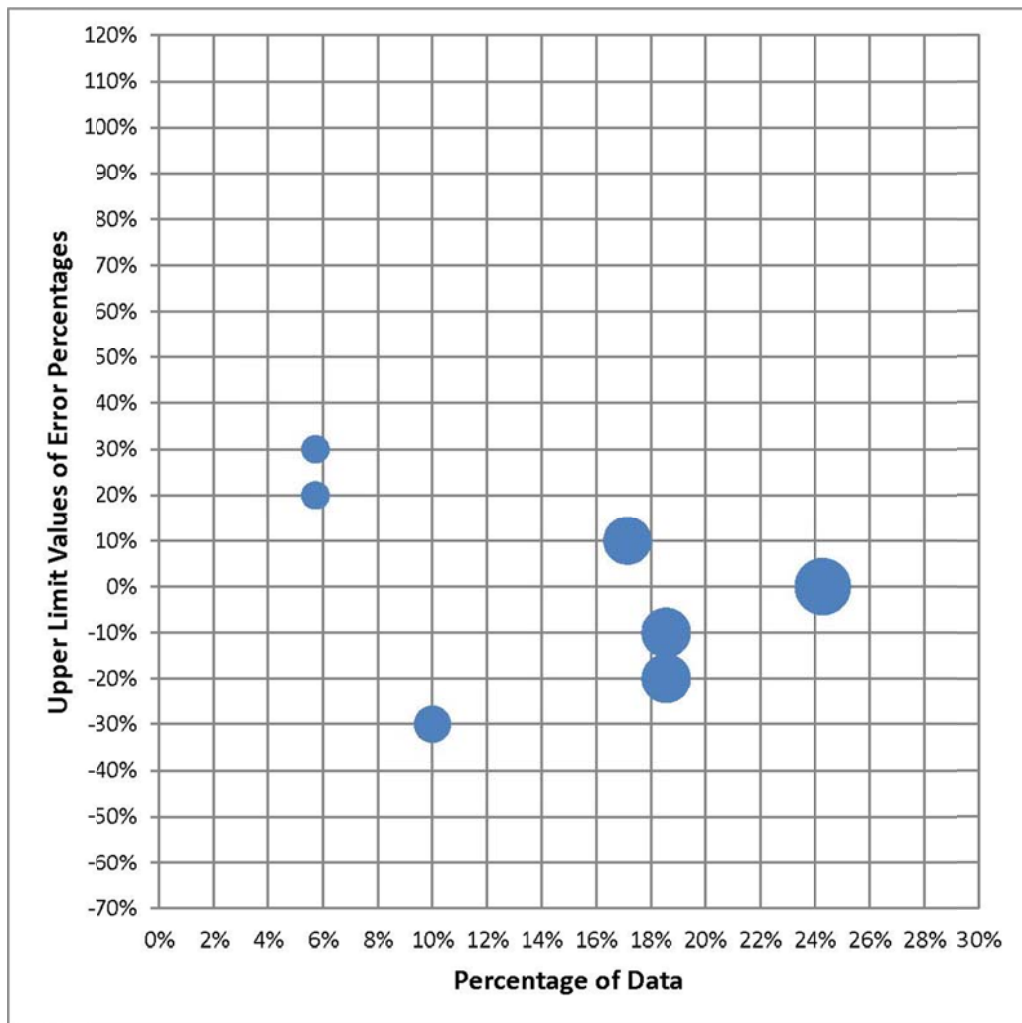
Figure 5.41 Number of data versus upper limit values of error percentages regarding the comparison of the S_c/D_i values calculated by Equation 5.9 and the measurements.
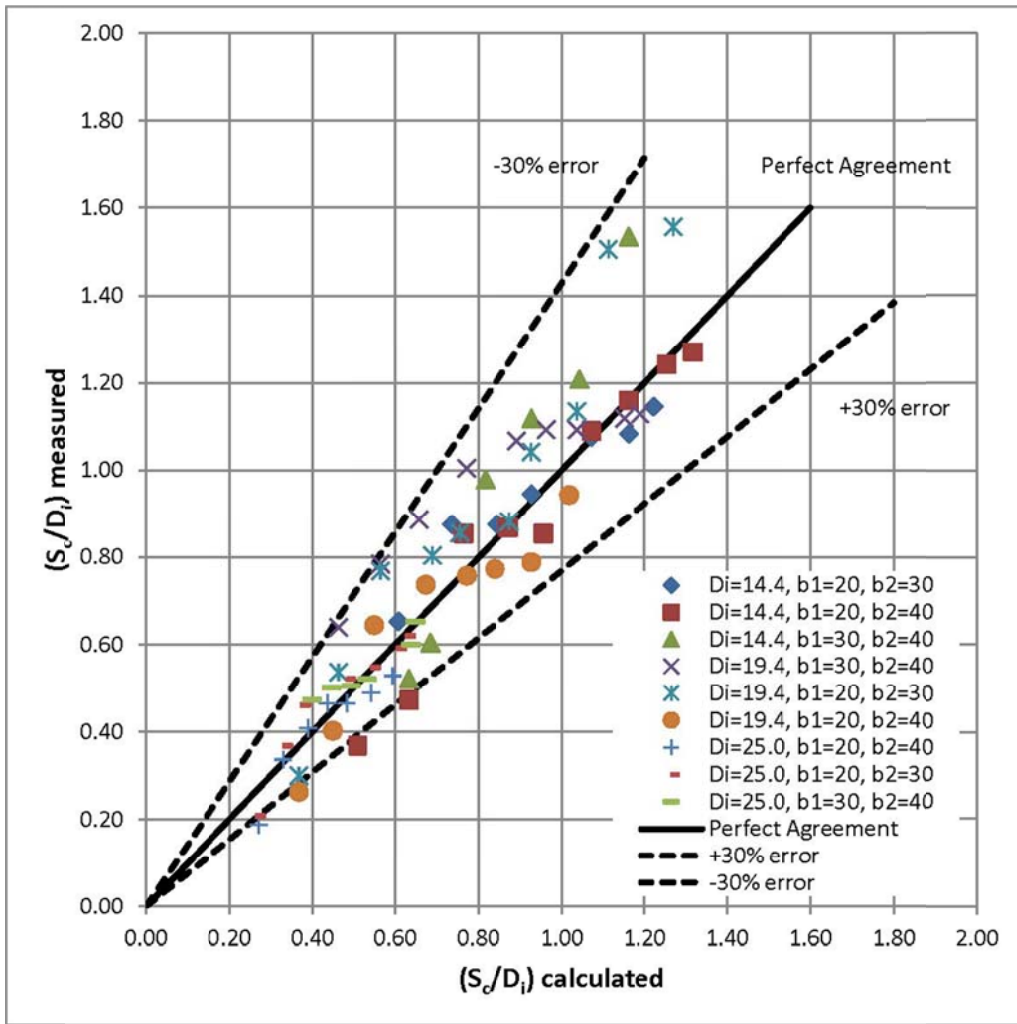
Figure 5.42 Comparison of the measured and calculated S_c/D_i values under influence of the dimensionless parameters mentioned in Equation 5.10
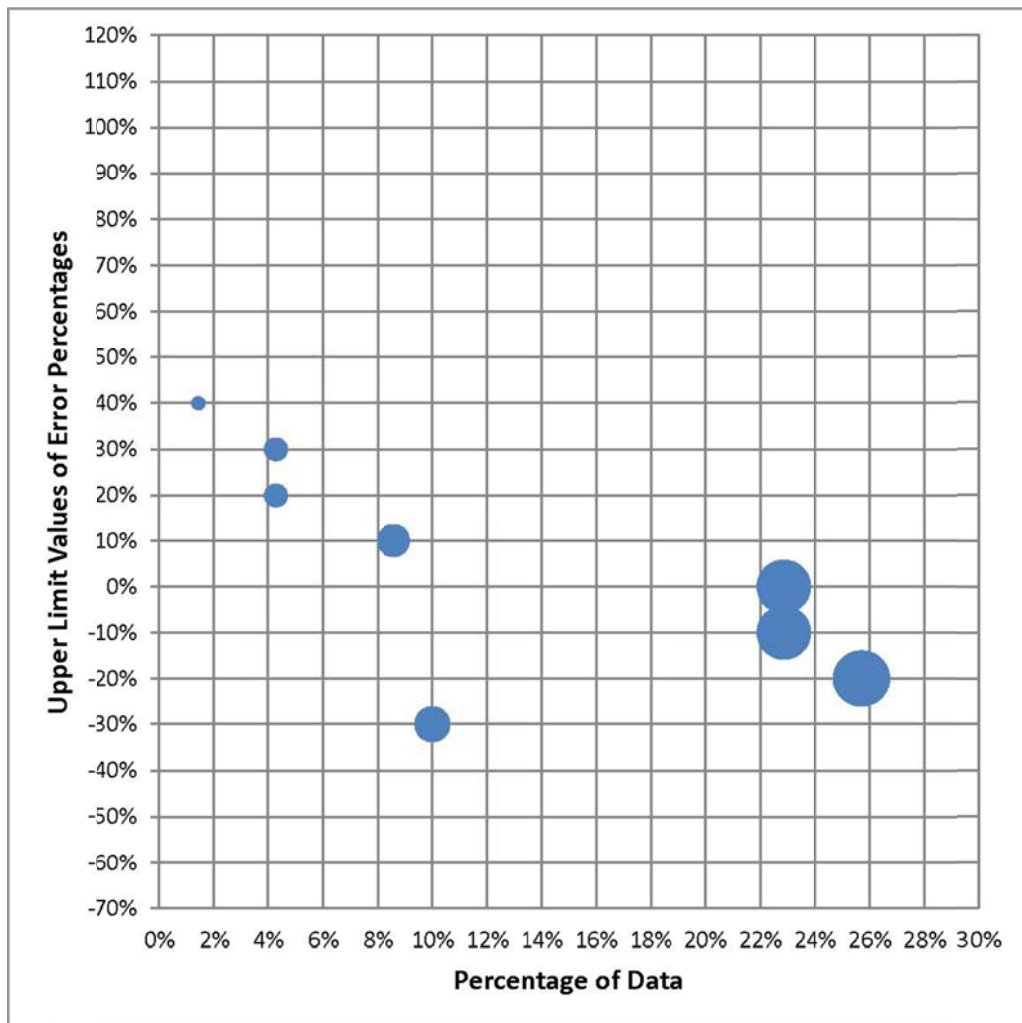
Figure 5.43 Number of data versus upper limit values of error percentages regarding the comparison of the S_c/D_i values calculated by Equation 5.10 and the measurements.

5.4. COMPARISON OF THE PRESENT EMPIRICAL EQUATIONS WITH THOSE SIMILAR ONES IN LITERATURE

5.4.1. Equation 5.2 versus Gürbüzdal's (2009) Relation

Gürbüzdal (2009) investigated the formation of air-entraining vortices in a horizontal intake model under symmetrical approach flow conditions with four pipes of different diameters. He presented an empirical equation (Equation 2.6) for S_c/D_i as a function of Fr, b/D_i and Re. In Equation 2.6, b denotes the side wall clearance measured from centerline of the intake pipe to one of the side walls in symmetrical approach flow conditions, and equivalent to $(b_1+b_2)/2D_i$ in this study.

To show the correlation between S_c/D_i values to be obtained from Equation 2.6 and Equation 5.2, using the Fr, Re, We, and b/D_i values of the experimental data provided from this study, the corresponding S_c/D_i values were determined and plotted with respect to each other in Figure 5.44. The predicted S_c/D_i values lie between ± 30 % error lines. These two equations can be considered compatible with each other. In this figure all units are in cm.
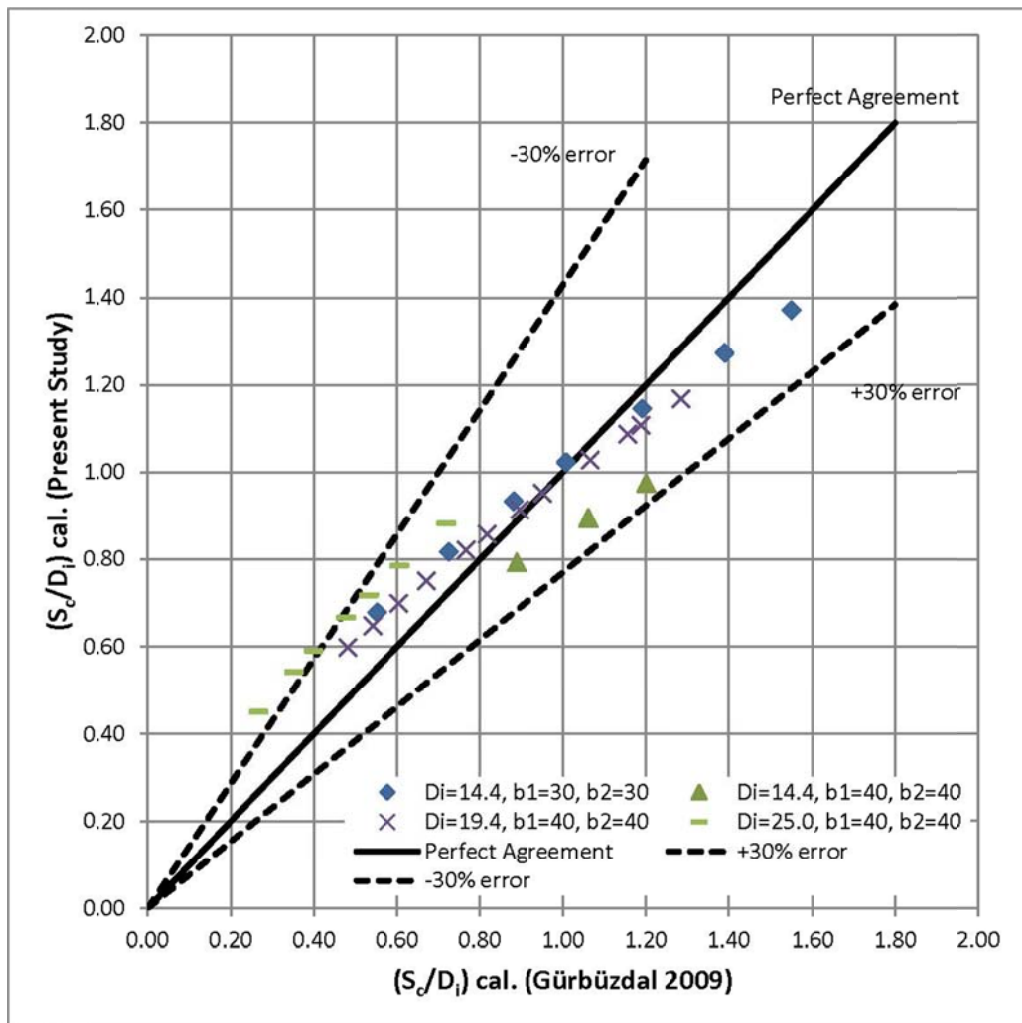
Figure 5.44 Comparison of calculated S_c/D_i values of Equation 5.2 versus Gürbüzdal 2009

5.4.2. Equation 5.2 versus Baykara's (2013) Relation

Baykara (2013) presented several emprical equations for S_c/D_i based on an experimental study conducted in the same model of the present study under symmetrical approach flow conditions with six pipes of different diameters and varying side wall clearances. Equation 2.9 is one of them which covers the similar ranges of the parameters used in this study.

To compare the S_c/D_i values of Equations 2.9 and Equation 5.2 the related dimensionless parameters of the present data were used and the calculated

69

S_c/D_i values were plotted in Figure 5.45. Figure 5.45 reveals that there is a good agreement between Equation 5.2 and Baykara's (2013) relation which lie within $\pm20\%$ error lines. In this figure all units are in cm.
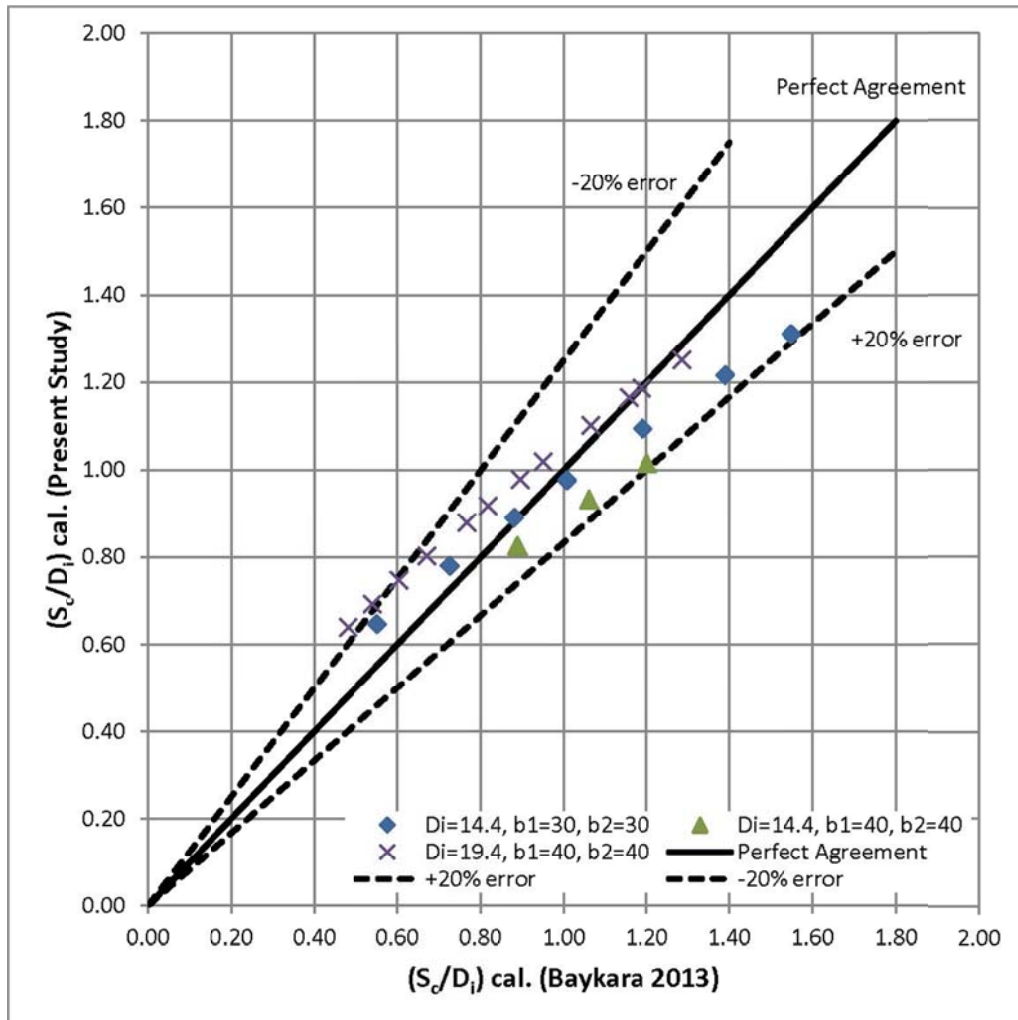
Figure 5.45 Comparison of calculated S_c/D_i values of Equation 5.2 versus Baykara 2013

5.4.3. Present Study versus Gordon's (1970), Reddy and Pickford's (1972) and Baykara's (2013) Studies

To compare the simplified forms of S_c/D_i relations obtained in this study as a function of only Froude number with the similar ones given in literature, Figure 5.46 was prepared. In this figure the plots of S_c/D_i values presented by

70

the above mentioned investigators and those given in Equation 5.5 and 5.10 in this study were shown.

Gordon's (1970) equations:

$$\frac{S_c}{D_i} = 1.70 Fr \qquad\qquad 5.11$$

for symmetrical approach flow conditions (Equation 2.1),

$$\frac{S_c}{D_i} = 2.27 Fr \qquad\qquad 5.12$$

for asymmetrical approach flow conditions (Equation 2.2)

Reddy and Pickford's (1972) equation (Equation 2.3):

$$\frac{S_c}{D_i} = 1 + Fr \qquad\qquad 5.13$$

Baykara's (2013) equations:

$$\frac{S_c}{D_i} = Fr^{0.639} \qquad\qquad 5.14$$

for symmetrical approach flow conditions (Equation 2.10),

$$\frac{S_c}{D_i} = 1.278\, Fr^{0.558} \qquad\qquad 5.15$$

which is valid for wide side wall clearances (Equation 2.12) under symmetrical approach flow conditions.

The Present Study:

$$\frac{S_c}{D_i} = Fr^{1.057} \qquad\qquad 5.16$$

for symmetrical approach flow conditions (Equation 5.5) and

$$\frac{S_c}{D_i} = Fr^{0.933} \qquad\qquad 5.17$$

for asymmetrical approach flow conditions (Equation 5.10)

Since most of the data used in plotting the curves given in Figure 5.46 based on the prototype and large scale model studies, except Baykara's (2013) data, one should not expect good correlations among all those curves given in the figure. The curves of the asymmetrical flows of the present study lies just above the one of the symmetrical flows as expected. The relations of the present data and Baykara's (2013) equation (Equation 5.14) underestimate S_c/D_i values compared to the other ones. The reason of this is neglecting the other dimensionless parameters; Re, We and $(b_1+b_2)/D_i$ from the original equations of S_c/D_i and having the data of small scale models. Whereas, Baykara's (2013) second equation, Equation 5.15, shows a good correlation with Gordon's relation for Froude numbers upto about 0.50~0.60. Because, Equation 5.15 was derived by using the data of the experiments in which the side wall clearances were large. Due to the strong scale effect, as stated by Baykara (2013), the S_c/D_i values obtained from the model studies must be multiplied by correction coefficients as a function of the model length scale. To provide the requested correction coefficients for known model length scales, more experiments should be conducted in models of large length scales. In this figure all units are in cm.
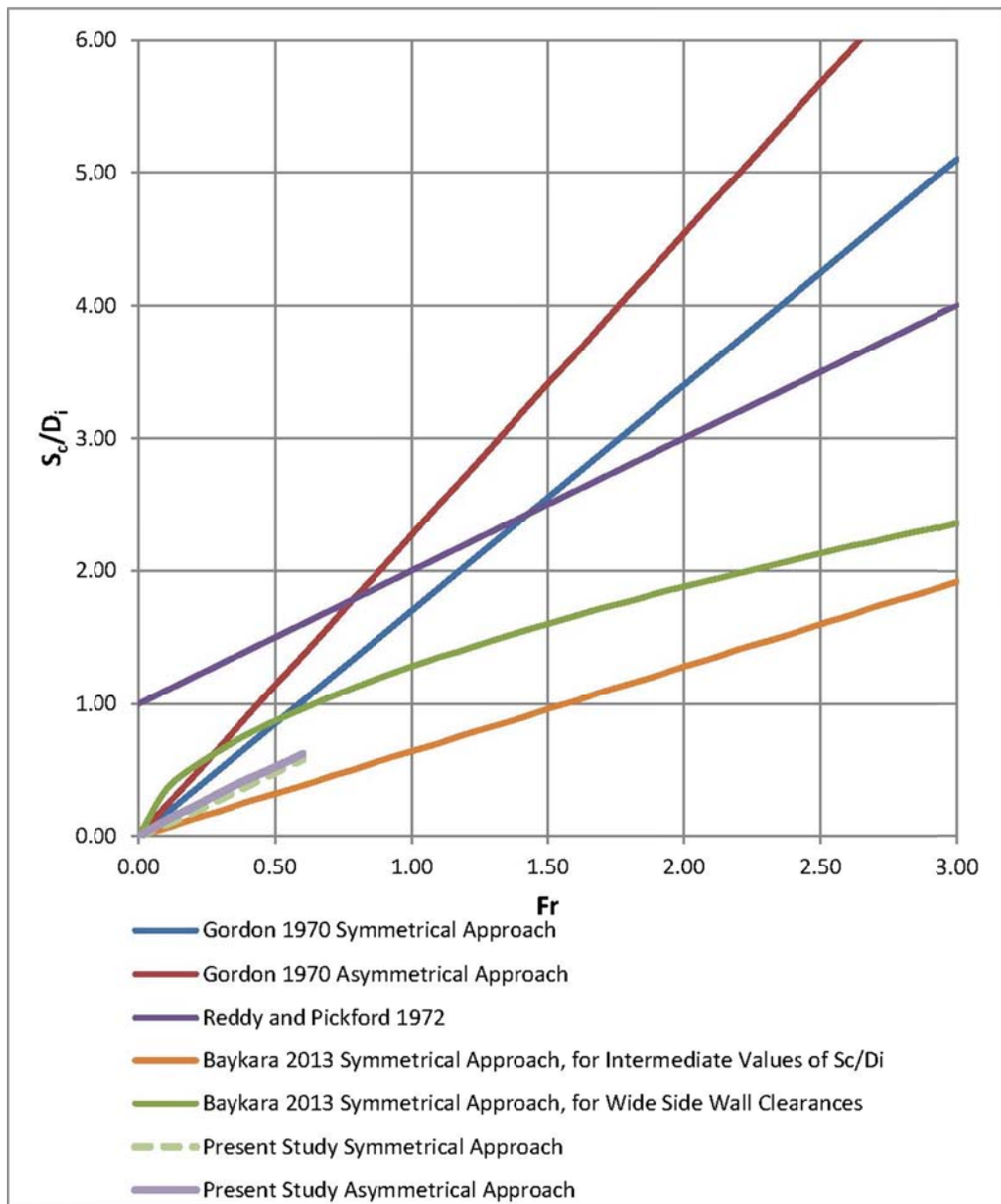
Figure 5.46 Plot of Fr versus S_c/D_i for different empirical equations in literature

CHAPTER 6

CONCLUSIONS AND RECOMMENDATIONS

Within the scope of this study the formation of air-entraining vortices in horizontal intakes were experimentally investigated for both symmetrical and asymmetrical approach flow conditions. Three pipes of different diameters were tested and empircal equations for the dimensionless critical submergence depth, S_c/D_i, were derived as a function of the related dimensionless parameters. From this study the following conclusions can be drawn:

1. For the intake pipes of known diameters, S_c/D_i values show an increasing trend with increasing values of Fr, Re and We for both symmetrical and asymmetrical approach flow conditions.

2. Empirical equations for S_c/D_i were derived as a function of Fr, Re, We, $(b_1+b_2)/D_i$ (for smmetrical approach flow conditions) and $|(b_1-b_2)|/D_i$ (for asymmetrical approach flow conditions) with high correlation coefficients.

3. Assymetrical approach flow conditions result in slightly larger dimensionless critical submergence depths for the ranges of parameters tested in this study.

4. The removal of some of the dimensionless terms; such as Re, We, $(b_1+b_2)/D_i$ or $|(b_1-b_2)|/D_i$ from the original equations of S_c/D_i does not affect the values of S_c/D_i significantly.

5. The relations drived for S_c/D_i from this study cannot be directly used to determine the corresponding prototype values of S_c/D_i for a given model length scale.

The following recommendations can be made for future studies:

1. Using more number of pipes at various diameters, the similar experiments should be repeated to get more generalized relations for S_c/D_i

2. Large scale model studies of prototype intakes should be made to determine the scale effect correction coefficients of S_c/D_i values. After that, one can easily convert the S_c/D_i values to be obtained from model studies to prototype values.

REFERENCES

Ahmad, Z., Rao, K.V. and Mittal, M.K. (2008), "Critical Submergence for Horizontal Intakes in Open Channel Flows", Department of Civil Engineering, Indian Institute of Technology Roorkee, India.

Anwar, H.O. (1965), "Flow in a Free Vortex", Water Power 1965(4), 153-161.

Anwar, H.O. (1967), "Vortices at Low Head Intakes", Water Power 1967(11), 455-457.

Anwar, H.O. (1968), "Prevention of Vortices at Intakes", Water Power 1968(10), 393-401.

Anwar, H.O., Weller, J.A. and Amphlett, M.B. (1978), "Similarity of Free-Vortex at Horizontal Intake", J. Hydraulic Res. 1978(2), 95-105.

Baykara, A., (2013), "Effect of Hydraulic Parameters on the Formation of Vortices at Intake Structures", M.S. Thesis, Civil Engineering Dept., METU.

Daggett, L.L. and Keulegan, G.H. (1974), "Similitude in Free-Surface Vortex Formations", J. Hydraulic Div., ASCE, HY11, 1565-1581.

Durgin, W.W. and Hecker, G.E. (1978), The Modeling of Vortices in Intake Structures. Proc IAHR-ASME-ASCE Joint Symposium on Design and Operation of Fluid Machinery, CSU Fort Collins, June 1978 vols I and III.

Gordon, J.L. (1970), "Vortices at Intakes", Water Power 1970(4), 137-138.

Gulliver, J.S. and Rindels, A.J. (1983), "An Experimental Study of Critical Submergence to Avoid Free-surface Vortices at Vertical Intakes", Project Report No: 224, University of Minnesota, St. Anthony Falls Hydraulic Laboratory.

Gürbüzdal, F., (2009), "Scale effects on the formation of vortices at intake structures", M.S. Thesis, Civil Engineering Dept., METU.

Jiming, M., Yuanbo, L. and Jitang, H. (2000), "Minimum Submergence before Double-Entrance Pressure Intakes", J. Hydraulic Div., ASCE, HY10, 628-631.

Knauss, J. (1987), "Swirling Flow Problems at Intakes", A.A. Balkema, Rotterdam.

Oakdale Engineering web site, http://www.oakdaleengr.com/download.htm, last accessed on 27.07.2014.

Reddy, Y.R. and Pickford, J.A. (1972), "Vortices at Intakes in Conventional Sumps", Water Power 1972(3), 108-109.

Taştan, K. and Yıldırım, N. (2010), "Effects of Dimensionless Parameters on Air-entraining Vortices", J. Hydraulic Research, 48:1, 57-64.

Yıldırım, N. and Kocabaş, F. (1995), "Critical Submergence for Intakes in Open Channel Flow", J. Hydraulic Engng., ASCE, 121, HY12, 900-905.

Yıldırım, N., Kocabaş, F. and Gülcan, S.C. (2000), "Flow-Boundary Effects on Critical Submergence of Intake Pipe", J. Hydraulic Engineering., ASCE, 126, HY4, 288-297.

Yıldırım, N., Taştan, K. and Arslan, M.M. (2009) "Critical Submergence for Dual Pipe Intakes", J. Hydraulic Research, 47:2, 242-249.

Zeigler, E.R. (1976), "Hydraulic Model Vortex Study Grand Coulee Third Powerplant", Engineering and Research Center, U.S Bureau of Reclamation, Denver, Colorado.

APPENDIX

EXPERIMENTAL RESULTS

Herein the experimental results in tabular form are given. Below figure explains the main variables that are mentioned in those tables.
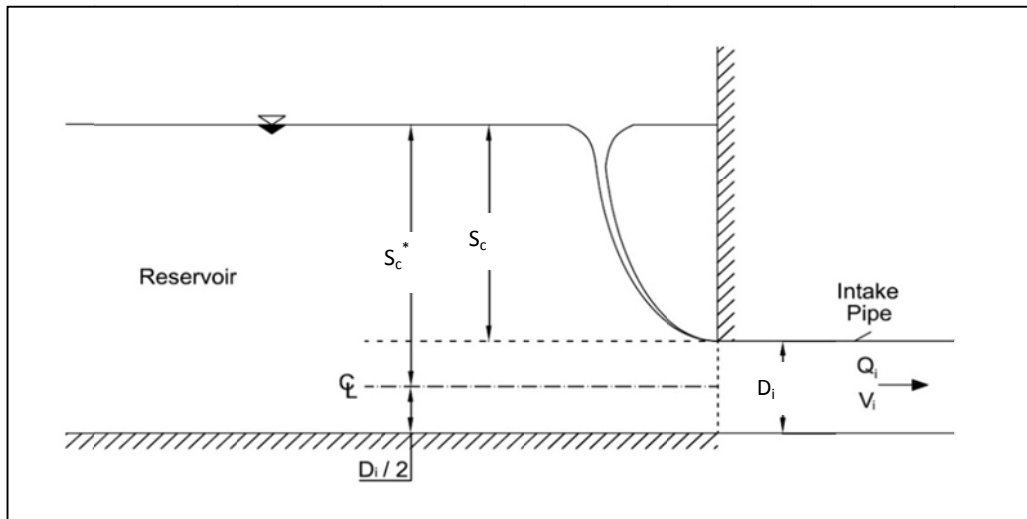
Figure A.1 Simple illustration of the critical submergence concept (Baykara 2013)

In order to obtain dimensionless numbers, the following parameters are used in the related formulas with the given values at 20^0 C:

$v =$ 1.004E-6 (m^2/s)
$\rho =$ 9.982E+2 (kg/m^3)
$\sigma =$ 7.28E-2 (N/m)

It should be noted that S_c is from summit point of the intake and S^*_c is from centerline of the intake, herein.

Table A.1 Critical submergence values obtained during the experiments for
D_i=14.4cm, b_1=30cm, b_2=30cm

Obs. No.	Q_i (lt/s)	S_c (cm)	S_c/D_i	V_i (m/s)	Fr	Re	We
1	11.34	6.50	0.451	0.696	0.586	99852	957
2	13.93	12.20	0.847	0.855	0.720	122669	1444
3	16.12	14.30	0.993	0.990	0.833	141993	1935
4	17.84	15.50	1.076	1.095	0.922	157109	2369
5	20.22	18.50	1.285	1.242	1.045	178096	3044
6	22.71	19.50	1.354	1.395	1.174	200034	3841
7	24.65	22.00	1.528	1.514	1.274	217111	4524

Table A.2 Critical submergence values obtained during the experiments for
D_i=14.4cm, b_1=20cm, b_2=30cm

Obs. No.	Q_i (lt/s)	S_c (cm)	S_c/D_i	V_i (m/s)	Fr	Re	We
8	11.34	9.40	0.653	0.696	0.586	99852	957
9	13.93	12.60	0.875	0.855	0.720	122669	1444
10	16.12	12.60	0.875	0.990	0.833	141993	1935
11	17.84	13.60	0.944	1.095	0.922	157109	2369
12	20.84	15.50	1.076	1.279	1.077	183492	3232
13	22.71	15.60	1.083	1.395	1.174	200034	3841
14	24.00	16.50	1.146	1.474	1.240	211359	4288

Table A.3 Critical submergence values obtained during the experiments for
D_i=14.4cm, b_1=20cm, b_2=20cm

Obs. No.	Q_i (lt/s)	S_c (cm)	S_c/D_i	V_i (m/s)	Fr	Re	We
15	9.39	7.60	0.528	0.576	0.485	82667	656
16	11.84	10.10	0.701	0.727	0.612	104296	1044
17	13.93	11.30	0.785	0.855	0.720	122669	1444
18	16.12	12.10	0.840	0.990	0.833	141993	1935
19	18.43	12.70	0.882	1.131	0.952	162267	2527
20	20.22	14.40	1.000	1.242	1.045	178096	3044
21	22.71	17.60	1.222	1.395	1.174	200034	3841
22	24.65	18.80	1.306	1.514	1.274	217111	4524
23	26.65	18.90	1.313	1.637	1.378	234723	5288
24	27.33	19.80	1.375	1.678	1.413	240712	5561

Table A.4 Critical submergence values obtained during the experiments for
D_i=14.4cm, b_1=20cm, b_2=40cm

Obs. No.	Q_i (lt/s)	S_c (cm)	S_c/Di	V_i (m/s)	Fr	Re	We
25	9.39	5.30	0.368	0.576	0.485	82667	656
26	11.84	6.80	0.472	0.727	0.612	104296	1044
27	14.47	12.30	0.854	0.888	0.748	127411	1558
28	16.69	12.50	0.868	1.025	0.863	146972	2073
29	18.43	12.30	0.854	1.131	0.952	162267	2527
30	20.84	15.70	1.090	1.279	1.077	183492	3232
31	22.71	16.70	1.160	1.395	1.174	200034	3841
32	24.65	17.90	1.243	1.514	1.274	217111	4524
33	25.98	18.30	1.271	1.595	1.343	228793	5024

Table A.5 Critical submergence values obtained during the experiments for
D_i=14.4cm, b_1=30cm, b_2=40cm

Obs. No.	Q_i (lt/s)	S_c (cm)	S_c/Di	V_i (m/s)	Fr	Re	We
34	11.84	7.50	0.521	0.727	0.612	104296	1044
35	12.87	8.70	0.604	0.790	0.665	113364	1234
36	15.56	14.10	0.979	0.956	0.804	137073	1803
37	17.84	16.10	1.118	1.095	0.922	157109	2369
38	20.22	17.40	1.208	1.242	1.045	178096	3044
39	22.71	22.10	1.535	1.395	1.174	200034	3841

Table A.6 Critical submergence values obtained during the experiments for
D_i=14.4cm, b_1=40cm, b_2=40cm

Obs. No.	Q_i (lt/s)	S_c (cm)	S_c/Di	V_i (m/s)	Fr	Re	We
40	16.12	13.30	0.924	0.990	0.833	141993	1935
41	18.43	14.20	0.986	1.131	0.952	162267	2527
42	20.22	15.80	1.097	1.242	1.045	178096	3044

Table A.7 Critical submergence values obtained during the experiments for
D_i=19.4cm, b_1=40cm, b_2=40cm

Obs. No.	Q_i (lt/s)	S_c (cm)	S_c/Di	V_i (m/s)	Fr	Re	We
43	20.22	10.10	0.521	0.684	0.496	132195	1245
44	22.08	12.10	0.624	0.747	0.542	144342	1484
45	24.00	16.80	0.866	0.812	0.589	156885	1754
46	25.98	19.80	1.021	0.879	0.637	169826	2055
47	28.71	19.10	0.985	0.971	0.704	187697	2510
48	30.12	21.50	1.108	1.019	0.739	196897	2762
49	32.28	19.80	1.021	1.092	0.792	211028	3173
50	33.76	18.10	0.933	1.142	0.828	220669	3469
51	36.79	18.80	0.969	1.245	0.903	240480	4120
52	39.13	19.30	0.995	1.324	0.960	255802	4662
53	39.93	22.10	1.139	1.351	0.980	260997	4853
54	42.35	20.30	1.046	1.433	1.039	276848	5461

Table A.8 Critical submergence values obtained during the experiments for
D_i=19.4cm, b_1=30cm, b_2=40cm

Obs. No.	Q_i (lt/s)	S_c (cm)	S_c/Di	V_i (m/s)	Fr	Re	We
55	17.84	12.40	0.639	0.604	0.438	116617	969
56	22.08	15.20	0.784	0.747	0.542	144342	1484
57	25.98	17.20	0.887	0.879	0.637	169826	2055
58	30.83	19.50	1.005	1.043	0.756	201563	2895
59	36.02	20.70	1.067	1.219	0.884	235461	3950
60	39.13	21.20	1.093	1.324	0.960	255802	4662
61	42.35	21.20	1.093	1.433	1.039	276848	5461
62	47.38	21.70	1.119	1.603	1.162	309740	6835
63	49.11	21.90	1.129	1.662	1.205	321057	7344

Table A.9 Critical submergence values obtained during the experiments for

D_i=19.4cm, b_1=30cm, b_2=30cm

Obs. No.	Q_i (lt/s)	S_c (cm)	S_c/Di	V_i (m/s)	Fr	Re	We
64	17.84	12.20	0.629	0.604	0.438	116617	969
65	23.35	15.80	0.814	0.790	0.573	152660	1660
66	27.33	15.70	0.809	0.925	0.671	178673	2274
67	30.12	15.20	0.784	1.019	0.739	196897	2762
68	33.76	15.60	0.804	1.142	0.828	220669	3469
69	38.34	16.70	0.861	1.297	0.941	250651	4476
70	42.35	17.20	0.887	1.433	1.039	276848	5461
71	45.68	17.20	0.887	1.545	1.121	298600	6352

Table A.10 Critical submergence values obtained during the experiments for

D_i=19.4cm, b_1=20cm, b_2=30cm

Obs. No.	Q_i (lt/s)	S_c (cm)	S_c/Di	V_i (m/s)	Fr	Re	We
72	13.93	5.80	0.299	0.471	0.342	91054	591
73	17.84	10.40	0.536	0.604	0.438	116617	969
74	22.08	14.90	0.768	0.747	0.542	144342	1484
75	27.33	15.60	0.804	0.925	0.671	178673	2274
76	30.12	16.60	0.856	1.019	0.739	196897	2762
77	35.26	17.10	0.881	1.193	0.865	230486	3785
78	37.56	20.20	1.041	1.271	0.922	245543	4295
79	42.35	22.00	1.134	1.433	1.039	276848	5461
80	45.68	29.20	1.505	1.545	1.121	298600	6352
81	52.66	30.20	1.557	1.781	1.292	344220	8442

Table A.11 Critical submergence values obtained during the experiments for
D_i=19.4cm, b_1=20cm, b_2=20cm

Obs. No.	Q_i (lt/s)	S_c (cm)	S_c/Di	V_i (m/s)	Fr	Re	We
82	15.56	4.50	0.232	0.527	0.382	101745	738
83	17.84	6.60	0.340	0.604	0.438	116617	969
84	21.45	9.10	0.469	0.726	0.526	140249	1401
85	25.98	10.60	0.546	0.879	0.637	169826	2055
86	30.83	15.20	0.784	1.043	0.756	201563	2895
87	34.50	22.50	1.160	1.167	0.847	225556	3625
88	38.34	25.00	1.289	1.297	0.941	250651	4476
89	42.35	28.50	1.469	1.433	1.039	276848	5461
90	46.53	33.30	1.716	1.574	1.141	304148	6591
91	49.99	56.90	2.933	1.691	1.226	326782	7608

Table A.12 Critical submergence values obtained during the experiments for
D_i=19.4cm, b_1=20cm, b_2=40cm

Obs. No.	Q_i (lt/s)	S_c (cm)	S_c/Di	V_i (m/s)	Fr	Re	We
92	13.93	5.10	0.263	0.471	0.342	91054	591
93	17.26	7.80	0.402	0.584	0.423	112833	907
94	21.45	12.50	0.644	0.726	0.526	140249	1401
95	26.65	14.30	0.737	0.902	0.654	174227	2163
96	30.83	14.70	0.758	1.043	0.756	201563	2895
97	33.76	15.00	0.773	1.142	0.828	220669	3469
98	37.56	15.30	0.789	1.271	0.922	245543	4295
99	41.54	18.30	0.943	1.405	1.019	271520	5252

Table A.13 Critical submergence values obtained during the experiments for
D_i=25.0cm, b_1=20cm, b_2=40cm

Obs. No.	Q_i (lt/s)	S_c (cm)	S_c/Di	V_i (m/s)	Fr	Re	We
100	19.02	4.70	0.188	0.387	0.247	96471	515
101	23.35	8.40	0.336	0.476	0.304	118464	776
102	28.02	10.20	0.408	0.571	0.365	142134	1117
103	31.56	11.60	0.464	0.643	0.411	160068	1417
104	35.26	11.60	0.464	0.718	0.459	178857	1769
105	39.93	12.20	0.488	0.813	0.520	202534	2268
106	44.00	13.20	0.528	0.896	0.573	223205	2754

Table A.14 Critical submergence values obtained during the experiments for
D_i=25.0cm, b_1=20cm, b_2=20cm

Obs. No.	Q_i (lt/s)	S_c (cm)	S_c/Di	V_i (m/s)	Fr	Re	We
107	19.02	3.30	0.132	0.387	0.247	96471	515
108	22.71	6.50	0.260	0.463	0.296	115220	734
109	27.33	6.00	0.240	0.557	0.356	138650	1063
110	31.56	9.30	0.372	0.643	0.411	160068	1417
111	35.26	10.40	0.416	0.718	0.459	178857	1769
112	39.13	14.10	0.564	0.797	0.509	198502	2178
113	43.17	15.80	0.632	0.880	0.562	219003	2652
114	47.38	26.00	1.040	0.965	0.617	240358	3194

Table A.15 Critical submergence values obtained during the experiments for
D_i=25.0cm, b_1=20cm, b_2=30cm

Obs. No.	Q_i (lt/s)	S_c (cm)	S_c/Di	V_i (m/s)	Fr	Re	We
115	18.43	5.20	0.208	0.375	0.240	93466	483
116	23.35	9.20	0.368	0.476	0.304	118464	776
117	26.65	11.50	0.460	0.543	0.347	135200	1011
118	31.56	12.50	0.500	0.643	0.411	160068	1417
119	35.26	13.00	0.520	0.718	0.459	178857	1769
120	39.93	13.70	0.548	0.813	0.520	202534	2268
121	44.84	14.80	0.592	0.913	0.584	227442	2860
122	46.53	15.50	0.620	0.948	0.606	236019	3080

Table A.16 Critical submergence values obtained during the experiments for
D_i=25.0cm, b_1=30cm, b_2=30cm

Obs. No.	Q_i (lt/s)	S_c (cm)	S_c/Di	V_i (m/s)	Fr	Re	We
123	23.35	11.50	0.460	0.476	0.304	118464	776
124	27.33	11.50	0.460	0.557	0.356	138650	1063
125	31.56	12.90	0.516	0.643	0.411	160068	1417
126	36.02	13.40	0.536	0.734	0.469	182718	1846
127	39.93	13.50	0.540	0.813	0.520	202534	2268
128	44.00	14.60	0.584	0.896	0.573	223205	2754
129	47.38	15.80	0.632	0.965	0.617	240358	3194

Table A.17 Critical submergence values obtained during the experiments for

D_i=25.0cm, b_1=30cm, b_2=40cm

Obs. No.	Q_i (lt/s)	S_c (cm)	S_c/Di	V_i (m/s)	Fr	Re	We
130	28.71	11.80	0.472	0.585	0.374	145653	1173
131	32.28	12.50	0.500	0.658	0.420	163758	1483
132	36.02	12.60	0.504	0.734	0.469	182718	1846
133	39.13	13.00	0.520	0.797	0.509	198502	2178
134	47.38	15.00	0.600	0.965	0.617	240358	3194
135	48.25	16.30	0.652	0.983	0.628	244732	3311

Table A.18 Critical submergence values obtained during the experiments for

D_i=25.0cm, b_1=40cm, b_2=40cm

Obs. No.	Q_i (lt/s)	S_c (cm)	S_c/Di	V_i (m/s)	Fr	Re	We
136	23.35	3.30	0.132	0.476	0.304	118464	776
137	28.71	4.10	0.164	0.585	0.374	145653	1173
138	31.56	9.00	0.360	0.643	0.411	160068	1417
139	36.02	12.00	0.480	0.734	0.469	182718	1846
140	39.13	13.30	0.532	0.797	0.509	198502	2178
141	43.17	14.90	0.596	0.880	0.562	219003	2652
142	49.11	17.20	0.688	1.001	0.639	249140	3432